FINAL TECHNICAL REPORT

PROJECT TITLE:	Novel Low Cost, High Reliability Wind Turbine Drivetrain
SOLICITATION TITLE:	U. S. Wind Power: Next Generation Drivetrain Development
REFERENCE NUMBER:	DE-FOA-0000439
AWARD NUMBER:	DE-EE0005141
PROJECT PERIOD:	09/11 – 06/12
LEAD ORGANIZATION:	Clipper Windpower, LLC 6305 Carpinteria Avenue, Suite 300 Carpinteria, CA 93013
TEAM MEMBERS:	United Technologies Research Center National Renewable Energy Laboratory Hamilton Sundstrand Corporation
TECHNICAL CONTACT:	Anthony Chobot (PI) Phone: (805) 576-1616; Fax: (805) 899-1115 Email: AChobot@ClipperWind.com
BUSINESS CONTACT:	Debarshi Das Phone: (805) 576-1321; Fax: (805) 745-5949 Email: DDas@ClipperWind.com
AUTHORS:	Anthony Chobot, Debarshi Das, Tyler Mayer, Zach Markey, Tim Martinson, Hayden Reeve, Paul Attridge, Tahany El-Wardany
DATE SUBMITTED:	September 13, 2012

Acknowledgment:

This report is based upon work supported by the U. S. Department of Energy under Award No. DE-EE0005141.

Disclaimer:

Any findings, opinions, and conclusions or recommendations expressed in this report are those of the author(s) and do not necessarily reflect the views of the Department of Energy.

EXECUTIVE SUMMARY

Clipper Windpower, in collaboration with United Technologies Research Center, the National Renewable Energy Laboratory, and Hamilton Sundstrand Corporation, developed a low-cost, deflection-compliant, reliable, and serviceable chain drive speed increaser.

This chain and sprocket drivetrain design offers significant breakthroughs in the areas of cost and serviceability and addresses the key challenges of current geared and direct-drive systems. The use of gearboxes has proven to be challenging; the large torques and bending loads associated with use in large multi-MW wind applications have generally limited demonstrated lifetime to 8-10 years [1]. The large cost of gearbox replacement and the required use of large, expensive cranes can result in gearbox replacement costs on the order of $1M, representing a significant impact to overall cost of energy (COE). Direct-drive machines eliminate the gearbox, thereby targeting increased reliability and reduced life-cycle cost. However, the slow rotational speeds require very large and costly generators, which also typically have an undesirable dependence on expensive rare-earth magnet materials and large structural penalties for precise air gap control. The cost of rare-earth materials has increased 20X in the last 8 years representing a key risk to ever realizing the promised cost of energy reductions from direct-drive generators. A common challenge to both geared and direct drive architectures is a limited ability to manage input shaft deflections.

The proposed Clipper drivetrain is deflection-compliant, insulating later drivetrain stages and generators from off-axis loads. The system is modular, allowing for all key parts to be removed and replaced without the use of a high capacity crane. Finally, the technology modularity allows for scalability and many possible drivetrain topologies. These benefits enable **reductions in drivetrain capital cost by 10.0%, levelized replacement and O&M costs by 26.7%, and overall cost of energy by 10.2%.**

This design was achieved by: (1) performing an extensive optimization study that determined the preliminary cost for all practical chain drive topologies to ensure the most competitive configuration; (2) conducting detailed analysis of chain dynamics, contact stresses, and wear and efficiency characteristics over the chain's life to ensure accurate physics-based predictions of chain performance; and (3) developing a final product design, including reliability analysis, chain replacement procedures, and bearing and sprocket analysis. Definition of this final product configuration was used to develop refined cost of energy estimates. Finally, key system risks for the chain drive were defined and a comprehensive risk reduction plan was created for execution in Phase 2.

Contents

EXECUTIVE SUMMARY iii

1 INTRODUCTION 1

1.1 Background 1
1.2 Innovative Clipper Chain Drive 2
1.3 Report Outline 2

2 CURRENT CHAIN DESIGNS AND STATE OF THE ART 3

2.1 Introduction 3
2.2 Current Chain Capabilities 4
2.3 Multi-Strand Load Share 4
2.4 Wear 4
2.5 Additional Design Parameters 4

3 CHAIN DRIVE TOPOLOGY OPTIMIZATION 5

3.1 Topology and Parameter Investigation 5
3.2 Optimization Study 6
3.3 Model Assumptions 6
3.4 Optimization Results Using Standard Design Rules 7
3.5 Optimization Results Using Aggressive Design Rules 7
3.5.1 Dual Stage - Aggressive Design Rules 8
3.5.2 Single Stage - Aggressive Design Rules 8
3.5.3 Hybrid - Aggressive Design Rules 8
3.6 Optimization Results Using Recommended Design Rules 9
3.6.1 Dual Stage - Recommended Design Rules 9
3.6.2 Single Stage - Recommended Design Rules 9
3.6.3 Hybrid - Recommended Design Rules 9
3.7 Configuration Down-Selection 11

4 DETAILED CHAIN ANALYSIS 12

4.1 Overview 12
4.2 Chain-Sprocket Dynamics System Modeling 13
4.2.1 First-Stage Chain Model 13
4.2.2 Transient Results 13
4.3 Finite-Element Modeling of Chain-Sprocket System 15
4.4 Wear and Efficiency Modeling 16
4.4.1 Prediction of Normalized Contact Area 17
4.4.2 Stribeck Friction Model 17
4.4.3 Wear Modeling and Prediction 18
4.4.4 Prediction of Chain Efficiency 18
4.4.5 Results 19

5 FINAL PRODUCT CONFIGURATION 19

5.1 General Overview 19

5.1.1 Key Design Features 21
5.2 Finite-Element Analysis 22
5.2.1 Sprocket Analysis 22
5.2.2 Main Support Plate Analysis 23
5.2.3 Results Summary 23
5.3 Shaft and Bearing Sizing 23
5.3.1 Bearing Analysis Results 24
5.3.2 Shaft Analysis Results 24
5.4 Operations and Maintenance (O&M) 24
5.5 Reliability – Current State versus Chain Drive (LRC) 25
5.5.1 Reliability Evaluation Methodology 25
5.5.2 Baseline Gearbox Reliability 25
5.5.3 Chain Drive Reliability 26
5.5.4 Generator Reliability Comparison 26
5.5.5 Reliability Comparison Summary 27
5.6 System Efficiency – Current State versus Chain Drive 27

6 COST OF ENERGY ANALYSIS 27

6.1 Summary of Baseline and COE Assumptions 27
6.2 COE Summary and Additional COE Improvements 31

7 RISK REDUCTION AND DEMONSTRATION PLAN 33

7.1 Key Technical Risk Areas 33
7.2 Technology Readiness Level (TRL) Analysis 34
7.3 Risk Reduction Plan 34
7.3 Sub-Scale Testing 36
7.3.1 Sub-Scale Test Objectives 36
7.4 Full-Scale Demonstrator Testing 36
7.4.1 Full-Scale Demonstrator Test Objectives 37
7.4.2 Full-Scale Demonstrator Test Facility 37
7.4.3 Full-Scale Demonstrator Test Article 37
7.4.4 Full-Scale Demonstration Test Plan 39
7.5 Revised Phase 2 Plan and Schedule 40
7.5.1 Project Management and Team Structure 40
7.5.2 Tasks to Be Performed 41
7.5.3 Project Schedule 42

8 REFERENCES 43

1 INTRODUCTION

This report summarizes Clipper Windpower's Phase 1 efforts under Contract DE-EE0005141 awarded in response to DE-FOA-0000439 that aims to develop next generation wind turbine drivetrains.

1.1 Background

In recent years, turbine manufacturers have increased rotor diameters, improved efficiency, enhanced controls, and coupled these technical advances with a keen focus on lowering costs to enable even greater penetration of wind power into the grid. The relentless push to reduce the overall cost of energy (COE) has led original equipment manufacturers (OEMs) and developers to focus on the full range of project costs including initial capital, assembly, transportation, development, balance of plant (BOP) and annual operations and maintenance (O&M). The wind turbine drivetrain typically makes up a significant proportion of the wind turbine capital cost, efficiency losses, and availability and repair impacts. In order to improve the performance of wind turbine drivetrains the Department of Energy's Next Generation Drivetrain Development program (DE-FOA-0000439) aims to achieve *"a 24% reduction in COE related to Levelized Replacement/Overhaul Costs (LRC) and Operations & Maintenance (O&M) costs, a 50% improvement in torque density (Nm/m^3) while maintaining an equivalent cost/torque, a 50% improvement in mean time between replacement of gearboxes and/or generators, and a 20% reduction in deployment cost"* [2].

The wind industry has traditionally used a geared drivetrain to increase rotational speed in order to minimize the size and capital costs of electrical generators. The use of gearboxes has proven to be very challenging; the large torques and bending loads associated with use in large multi-megawatt wind applications have generally limited demonstrated lifetime to 8-10 years despite advertised 20-year design life [1]. Given the large cost of gearbox replacement and the required use of large, expensive cranes that can drive gearbox replacement costs on the order of $1M, the portion of COE attributable to a gearbox considering all life cycle costs is significant. These challenges and their associated costs have led the wind turbine community to consider a number of alternative approaches.

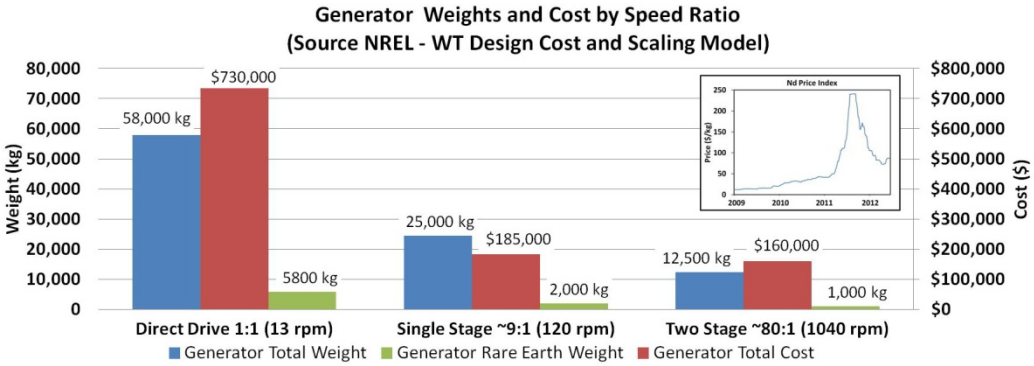

Figure 1: Generator and rare-earth weights and generator cost versus speed ratio for 2.5 MW design; rare-earth cost history (inset) [31].

The most popular alternative approach is the direct-drive machine that eliminates the gearbox, thereby targeting increased reliability and life cycle cost reduction. However, the slow rotational speed requires very large and costly generators, which also typically have an undesirable dependence on expensive rare-earth magnet materials [3] and large structural penalties for

precise air gap control. Figure 1 shows generator costs and weight and rare-earth weight versus speed for a typical 2.5 MW permanent magnet machine. Rare-earth costs have risen dramatically, increasing 20X in the last 8 years, also shown in Figure 1.

1.2 Innovative Clipper Chain Drive

The wind industry needs not only a direct-drive solution, which simply transfers cost and size disadvantages from the gearbox to the generator, but a speed increaser that is low cost, reliable, efficient, and serviceable. Clipper Windpower proposes an innovative drivetrain involving the use of **chains and sprockets as a low-cost, deflection-compliant, reliable and serviceable speed increaser.** This technical approach leverages technology developed and demonstrated in United Technologies Corporation's Otis division, the world leader in escalators and elevators, and is currently used in escalators around the world. The Otis experience is extensive; chain and sprocket drives power over 70,000 Otis escalators around the world with a cumulative run time of over 4 billion hours. Figure 2a shows a typical chain drive in an escalator, where key criteria are reliability and affordability, goals that align directly with the wind industry.

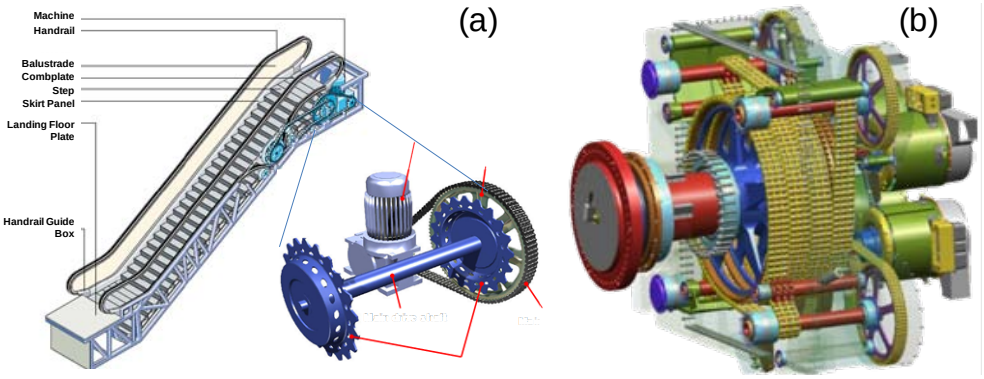

Figure 2: Chain drive in an (a) Otis escalator and (b) example wind turbine drivetrain.

Figure 2b shows an example design concept for a 2.5MW drivetrain using a chain and sprocket for both the first and second stage. In this design the rotor drives a large sprocket that engages multiple chain strands. These strands drive four first-stage sprockets connected to second-stage sprockets, which in turn drive four high speed generator output shafts. This concept allows increased speed to minimize generator weight while **eliminating the large and costly gearbox.** The chain and sprocket approach is inherently tolerant to shaft misalignment, does not require precision ground gears, and is thus much less complex and less costly.

1.3 Report Outline

The remainder of this report documents Clipper Windpower's Phase 1 investigation and comprises three main elements. The first element, engineering design process, is covered in Sections 2-5. Section 2 documents current chain design practices and state-of-the-art capability. Section 3 documents the chain drive topology optimization process, detailing how parametric models were used to optimize against key COE metrics to determine the preferred number of stages, speed ratios, etc. Section 4 describes the chain drive analysis performed by UTRC including dynamic, finite element, and analytical analysis of loads, wear, and efficiency. Section 5 describes Clipper's conceptual engineering design and analysis for a multi-megawatt chain drive system. The second element, cost of energy (COE) analysis, assumptions, and rationale, is presented in Section 6. The third element, the proposed Phase 2 risk reduction and testing plan, is presented in Section 7.

2 CURRENT CHAIN DESIGNS AND STATE OF THE ART

2.1 Introduction

Chain has been in use in engineering systems in various forms for centuries and is generally categorized by application: conveyor, tension, or transmission. Conveyor chain slides or rolls along a horizontal surface and is responsible for material transport. Tension chain is used in applications such as fork lift mechanisms where the chain is not a continuous loop and operating speeds are very low. Transmission chains are the category of interest for wind turbine applications. AISI established a specification, B29-100 [4], which was later adopted and is currently maintained by ASME. This specification allows interchangeability of chains and sprockets by defining formulas for standard profiles.

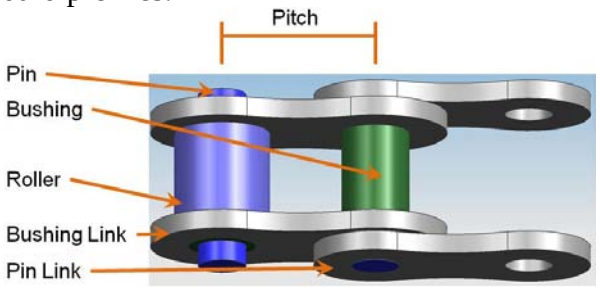

Figure 3: Features of straight link transmission chain.

There are two types of links in a straight link chain (Figure 3). Pin-links have pins press fit into them. Bushing-links have bushings press fit into them. As links articulate, sliding occurs between the pin and bushing. The roller/bushing is also a sliding interface. A number of different chain options are described below:

Offset Link Chain: Straight link chain does not have even wear distributed along the chain. As wear is accumulated, the chain develops two different pitch lengths that the chain system must accommodate. A potential solution, offset link chain, has a more uniform wear distribution, improving wear life. However, for equal load capacity chain, offset links will tend to be larger. This can be problematic for chain dynamics and impact as links and sprocket come in and out of contact. No offset link chain was found capable of the load levels required for multi-megawatt wind turbine applications.

Double Pitch Chain: Double pitch chain has longer links, doubling the standard pin center-to-center spacing. This is more commonly found in conveyor chains.

Engineering Chain: "Engineering chain" has geometry intended for very coarse environments such as earth moving equipment, allowing material to freely engage and dislodge in the transmission. The wide clearances in the sprocket form are not appropriate for wind turbines, or any machine requiring backlash control.

Heavy Link Chain: Manufacturers also offer a heavy link chain option in which the link plate thickness for a given chain pitch is equal to the next size up in the standard table. The link will also have a more straight side profile for increased link load capacity. While beneficial for fatigue, wear life is not improved.

Multi-Strand Chain: A last variation of note is single versus multi-strand chain (Figure 4), which typically combines up to six chain strands and enables larger capacity for power transmission.

2.2 Current Chain Capabilities

Chain sizing and selections are generally made through consultation of horsepower tables found in design standard such as ANSI B29.100 or manufacturers proprietary rating tables. In addition to the basic "standard" series chains, most manufacturers offer various grades of steel chain to help machine designers balance cost versus durability. For example, a major chain manufacturer offers a standard ANSI series steel chain and also offers other grades that improve characteristics such as fatigue or maximum allowable working load. These other chains can offer an additional 45% in load capacity and 55% in fatigue life beyond the basic series chain.

2.3 Multi-Strand Load Share

The load capacity of six-strand chain is typically not six times that of a single strand. This is due to the way that the chain is assembled. While the outer links are press fit to their pins and bushings, the links in the interior typically are slip fit for assembly. This clearance must be taken up via bending in the pins and bushings as load redistributes. This results in a de-rating or load capacity factor (Figure 4). Manufacturers have suggested that interior links may also be press fit, allowing close to 100% load sharing between strands. This has a cost and complexity impact. If done at room temperature, concern arises for the pin surface quality after assembly. Shrink fitting by heating the links and chilling the pins/bushings may mitigate this.

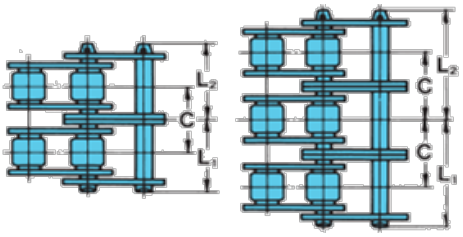

# Strands	Multiple Strand Load Capacity Factor
1	1
2	1.7
3	2.5
4	3.3
5	4.1
6	4.9

Figure 4: Multi-strand chain (left) and typical multi-strand load capacity reductions (right) [16].

2.4 Wear

As the chain drive operates, frictional sliding interfaces will wear, causing the meshing geometry to change. The effective pitch of the chain increases and the point of contact between the roller and the sprocket will tend to rise out of the valley of the sprocket, moving further up on the teeth. This leads to higher bending loads on sprocket teeth leading to tooth fatigue failures. Greater slack will arise in the slack side of the chain loop. Left long enough, in an advanced state of wear, the chain can eventually climb above the sprocket teeth and skip.

Wear is managed by monitoring chain elongation and replacing chain well before these problems arise. Typically when 1.5% elongation is accumulated, the chain is retired. For configurations using greater than 120 teeth, lower levels of elongation are required since more links are engaged with the larger sprocket.

Wear at the pin/bushing interface is the only zone that contributes to pin centerline to centerline shift. This is a surrogate for all wear interfaces. While wear also occurs at the bushing/roller and roller sprocket zones, they do not contribute to the elongation measurement. The pin/bushing also has the most concentrated contact stress of the sliding interfaces.

2.5 Additional Design Parameters

Detail design of a chain system must also take into account other design parameters such as operating environment, temperatures, lubrication, alignment, and orientation. For example, an additional de-rating factor may be applied for applications in extreme cold or hot environments.

Additionally, the load and speed will indicate the type of lubrication required; from slow, lightly loaded dry running chains to drip, bath, or jetted application of lubricating fluid.

3 CHAIN DRIVE TOPOLOGY OPTIMIZATION

3.1 Topology and Parameter Investigation

The goal of the optimization study was to determine the preferred chain-based topology and associated wind turbine specification. The high-level turbine configuration parameters are based on the Liberty 2.5 MW wind turbine drivetrain requirements:

- 2.5 MW nominal power rating
- 2.75 MW (3,684 hp) input drive rating
- 1,692 kNm (1,248,000 ft.lbs) input torque
- 15.5 RPM input speed
- 91% drivetrain efficiency (including electrical system losses)

The chain topologies investigated in this study include a single-stage chain drive, two-stage chain drive, and a 'hybrid' first-stage chain with second stage gearbox (Figure 5). Key design parameters were tooth count, speed ratio, number of strands, number of stages, number of torque splits, and load sharing factors. Using these design parameters this optimization determined the preferred chain-based topology for maximum overall wind turbine COE reduction.

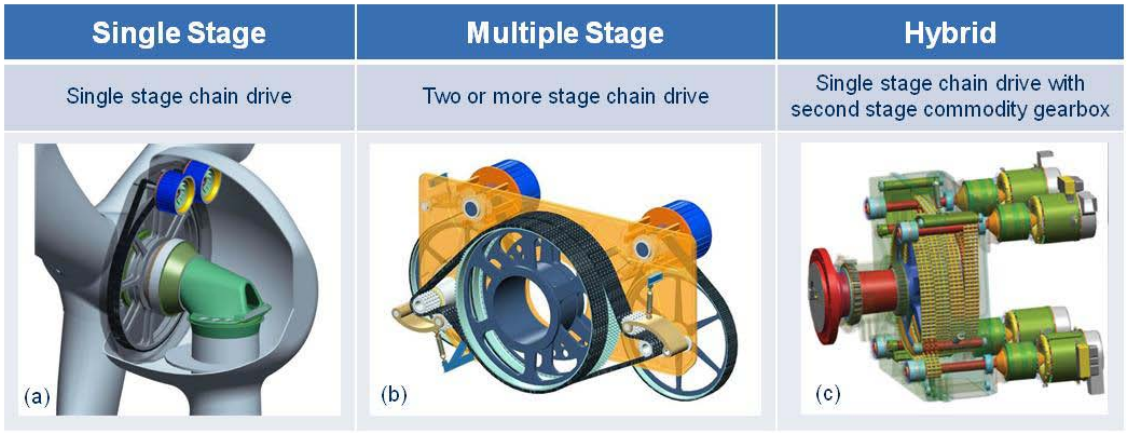

Figure 5: Example chain drive topologies: (a) Single Stage with large diameter sprocket; (b) Dual Stage (c) Hybrid chain drive with modular gearbox and generator units.

In addition to the three topologies, the impact of "Standard" and "Aggressive" design rules was evaluated. The Standard design criterion (Section 3.4) uses the basic ratings and design rules directly from ANSI B29.100 [4]. The Aggressive design criterion (Section 3.5) assumes that new technologies and improved analysis will allow future designs to significantly exceed the limitations of standard design rules. The main areas of improvement in the aggressive design rules are increased load capacity of the chains, better load sharing between strands, and improved wear performance. Finally, a "Recommended" set of design rules (Section 3.6) was evaluated to temper the aggressive design with practical design limits with an aim to improve likelihood of success and commercialization potential. In Figures 6 to 11 the recommended design criteria were used as a basis for comparison. Table 1 below outlines the parameter variation for each approach in the optimization study.

Table 1: Comparison of optimization parameter limits for different design rules.

Optimization Parameters	Standard Rules	Aggressive Rules	Recommended Rules
Chain Pitch	100-240 ANSI (Standard)	100-240 ANSI (Manufacturer)	100-240 ANSI (Manufacturer)
Horsepower Rating	ANSI B29.1 Standard	Manufacturer Advanced	Manufacturer Advanced
# of Strands	6 Max	6 Max	6 Max
Multi Strand De-Rating	Included	Not Included	40% of Standard
Torque Splits / # Outputs	1-10	1 - 10	1 - 4
Ratio	7:1 Max	> 40:1	12:1 Max
Large Sprocket # Teeth	120 Max	400 Max	200 Max
Small Sprocket # Teeth	9 Min	9 Min	17 Min

It is important to note the aggressive and recommended design rules may not be met with standard off-the-shelf chain. These designs may need to employ technology enablers to become viable products. For example, large sprocket tooth counts of greater than 120 may require special wear-resistant chains to last reasonable life cycles. Multi-stranded chains may require improved load sharing technology to achieve the increased capacity.

3.2 Optimization Study

Drivetrain component cost is a significant contributor to wind turbine cost of energy. The optimization study presented here seeks to find the greatest impact on COE by determining the lowest cost of the thousands of possible chain drive architectures. This was accomplished by iterating through the following steps for each possible combination:

1. Perform the design calculations for a chain drive system
2. Determine the length of chain
3. Determine the diameters and weights of the sprockets
4. Estimate cost of the chain drive components
5. Determine the speed and cost of the generator

The optimization study was performed using a macro-enabled Excel spreadsheet. The main optimization was on all possible combinations of large and small sprocket number of teeth. These two parameters define the ratio, speed, and load capacity of the chain and by using these values the entire system can be defined. In addition, adjustable parameters for chain pitch, number of torque splits, number of strands, de-rating factor, service factor, generator cost ratio factor, and additional chain performance factor were used to perform all chain design calculations and determine the lowest cost system. For each topology the entire parameter space was evaluated to understand the influences of each component and calculation on the system cost and mass. The output values of the study are the total cost of the power transmission components (sprockets, chains and generators) for each possible speed ratio.

3.3 Model Assumptions

The optimization model performed all the relevant calculations to determine the approximate cost for the power transmissions components (chains, sprockets, and generators) of the chain drive. The calculations were performed using the following assumptions:

Housing Bearings and Shafts: The housings, bearings, and shafts are assumed to be the same between configurations. Detailed assessment is provided for the preferred concept in Section 5.
Chain Ratings: The chain horsepower ratings are taken directly from ANSI B29.100 and from commercially available literature. An “Additional Chain Performance” factor is available to

account for superior chain performance from using a major manufacturer's high performance chains. The additional cost of using these chains is not considered at this stage of the analysis.

Multi-Strand Load Factor: Current standard and manufacturers' design recommendations call for a de-rating of multiple chain strands. Through advanced sprocket or chain design it may be possible to reduce or eliminate this de-rating. A factor is built into the spreadsheet to adjust the level of de-rating used in the optimization: 100% uses the full de-rate and 0% does not de-rate at all. The corresponding load factor is multiplied by the single strand load capacity to determine the multi-strand chain load capacity.

Chain Mass and Cost: The chain cost is based on distributors' catalogue prices that were averaged and then discounted by a "volume price factor" of 50% which was considered reasonable based on discussions with a chain manufacturer. The length of chain required for each configuration was determined by the diameters of the sprockets. This is a close approximation of the minimum chain required; this does not include any idlers and is likely to be lower than the actual chain length.

Sprocket Mass and Cost: The cost of the sprockets is assumed to be proportional to the mass. The mass is calculated by determining the volume of the sprocket teeth and by preliminary modeling of a sprocket hub in CAD. The sprockets were modeled at various diameters and curve fit to create continuous functions for interpolation.

Generator Cost: The generator cost used in the optimization study was calculated based on data from multiple generator manufacturers for many different generator speeds at the 2.5 MW level. A scaling factor was used to correlate the study curve to a reasonable current cost based on Clipper sourcing experience. This factor can be adjusted to determine the sensitivity of the designs to rare-earth magnet price fluctuations.

Hybrid/Gearbox Cost: The gearbox cost of the hybrid configuration is estimated using budgetary pricing of an off-the-shelf industry gearbox of similar scale. The costs of the other higher torque gearbox models are approximated by scaling from this value.

System Costs: The costs generated from the optimization spreadsheet are estimations and are not to be considered accurate bill-of-material costs. However, since all configurations are evaluated under the same criteria the relative cost differential between configurations is valid. More refined system costs for the preferred topology are provided in Section 5.

3.4 Optimization Results Using Standard Design Rules

The standard design rules generate topologies that are too unwieldy for practical consideration. Each configuration is more expensive than the baseline by a substantial amount. In addition to the high costs, the large number of torque paths, strands of chains, and components create an overly complex drivetrain. Even though the single-stage topology is less complex than the dual stage, its low speed ratio results in large and expensive generators. Due to these considerations the standard design rules did not yield any drivetrains fit for further consideration.

3.5 Optimization Results Using Aggressive Design Rules

The aggressive design rules allow consideration of increased large-sprocket tooth counts and increased chain load capacity, generating a multitude of lower cost drivetrain candidates. The optimal solution for each topology option is presented below. In general, these designs are optimum at the boundaries of the aggressive design rules. However, the optimal layouts at these design limits have practical challenges that are not captured in the parametric model, such as number of stages and number of outputs as well as overall size.

3.5.1 Dual Stage - Aggressive Design Rules

This option has the lowest capital cost of all configurations studied. However, its six power outputs increases complexity, part count, and packaging issues. Furthermore, the 11-tooth small sprocket will have high variations in chain tension (known as chordal action).

	Stage 1	Stage 2	Meets Rec. Design Rules?	
Chain Pitch (in)	2	1.25	≤3	Y
# of Strands	6	6	Less is better	Y
Large Sprocket Teeth	114	182	≤200	Y
Small Sprocket Teeth	11	26	≥17	N
Chain length (ft)	28	21.3	Less is better	Y
Ratio	10.36:1	7	≤12 per stage	Y
# Outputs	6	6	≤4	N
Large Sprocket Diameter	1.9m	1.7m	≤4.2m	Y

Figure 6: Summary of optimal two-stage topology based on aggressive design rules.

3.5.2 Single Stage - Aggressive Design Rules

This large diameter, high speed-ratio, single-stage design eliminates the complexity of multiple stages. The design features an innovative support structure that allows for a large diameter sprocket without heavy webs. However, the six outputs add complexity and the 758-tooth large sprocket is very large and may impact chain life. Finally, at nearly 8 meters in diameter, expensive shipping or onsite assembly would be required.

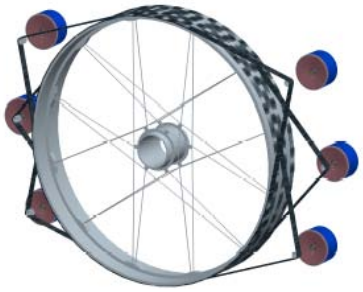

	Stage 1	Meets Rec. Design Rules?	
Chain Pitch (in)	1.25	≤3	Y
# of Strands	6	Less is better	Y
Large Sprocket Teeth	758	≤200	N
Small Sprocket Teeth	17	≥17	Y
Chain length (ft)	83	Less is better	Y
Ratio	42.11:1	≤12	N
# Outputs	6	Less is better	N
Large Sprocket Diameter	7.8m	≤4.2m	N

Figure 7: Summary of optimal single-stage topology based on aggressive design rules.

3.5.3 Hybrid - Aggressive Design Rules

The final topology incurs just one chain stage and utilizes modular gearboxes for the second stage. These gearboxes are replaceable with on-board cranes ensuring easy field servicing. The optimal speed ratios for this topology do still result in larger and more expensive generators. Like the above concepts the 11-tooth small sprocket may cause chordal and dynamic issues and the 4.5 m diameter will require either expensive shipping or field assembly, both of which add to the overall cost.

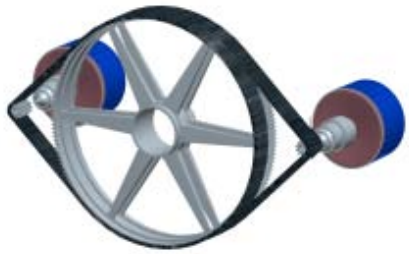

	Stage 1	Gearbox	Meets Rec. Design Rules?	
Chain Pitch (in)	3		≤3	Y
# of Strands	6		Less is better	Y
Large Sprocket Teeth	182		≤200	Y
Small Sprocket Teeth	11		≥17	N
Chain length (ft)	36.5		Less is better	Y
Ratio	16.55	7.02	≤12 per stage	N
# Outputs	2	2	Less is better	Y
Large Sprocket Diameter	4.5m	<1m	≤4.2m	N

Figure 8: Summary of optimal hybrid topology (chain first stage, gearbox second stage) based on aggressive design rules.

3.6 Optimization Results Using Recommended Design Rules

The recommended design rules were implemented to eliminate the concerns present in all of the above designs. In this scenario the design rules were set to achieve a lower overall level of technical risk in exchange for a slightly higher cost than the absolute minimum possible. In this scenario, the optimization yields practical designs for the dual stage and hybrid configurations that still have a significantly lower cost than the baseline. However, using these design criteria the single stage configuration is substantially more expensive.

3.6.1 Dual Stage - Recommended Design Rules

The results using the recommended design rules show that the two-output dual-stage design has a competitive cost with many other desirable features. The two outputs have a low part count and decreased packaging complexity. The overall architecture will be shippable as a complete unit.

	Stage 1	Stage 2	Meets Rec. Design Rules?	
Chain Pitch (in)	3	1.75	≤3	Y
# of Strands	5	6	Less is better	Y
Large Sprocket Teeth	148	200	≤200	Y
Small Sprocket Teeth	17	35	≥17	Y
Chain length (ft)	40	32.6	Less is better	Y
Ratio	8.71	5.71	≤12 per stage	Y
# Outputs	2	2	Less is better	Y
Large Sprocket Diameter	3.7m	2.8m	≤4.2m	Y

Figure 9: Summary of optimal two-stage topology based on recommended design rules.

3.6.2 Single Stage - Recommended Design Rules

The single-stage design is severely handicapped by the recommended design rules. With the practical limitations on maximum and minimum number of teeth, the greatest achievable ratio is 12:1. This results in a generator that is too costly to compete with the higher speed offerings.

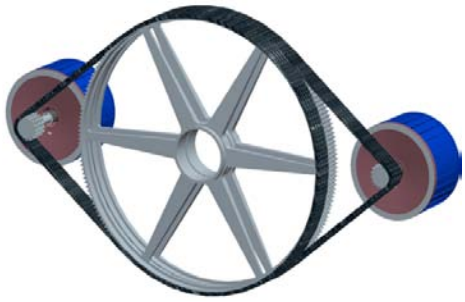

	Stage 1	Meets Rec. Design Rules?	
Chain Pitch (in)	3	≤3	Y
# of Strands	4	Less is better	Y
Large Sprocket Teeth	200	≤200	Y
Small Sprocket Teeth	17	≥17	Y
Chain length (ft)	40	Less is better	Y
Ratio	11.76	≤12 per stage	Y
# Outputs	2	Less is better	Y
Large Sprocket Diameter	4.81m	≤4.2m	N

Figure 10: Summary of optimal single-stage topology based on recommended design rules.

3.6.3 Hybrid - Recommended Design Rules

The recommended design rules show the hybrid topology having the lowest capital cost. The dual outputs reduce complexity and the high speed generators significantly reduce total cost.

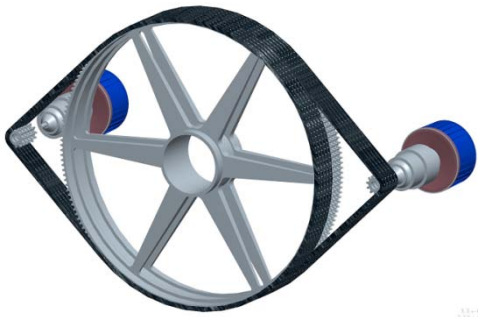

	Stage 1	Gearbox	Meets Rec. Design Rules?	
Chain Pitch (in)	3		≤3	Y
# of Strands	5		Less is better	Y
Large Sprocket Teeth	165		≤200	Y
Small Sprocket Teeth	17		≥17	Y
Chain length (ft)	35.5		Less is better	Y
Ratio	9.71	11.96	≤12 per stage	Y
# Outputs	2	2	Less is better	Y
Large Sprocket Diameter	4.0m	<1m	≤4.2m	Y

Figure 11: Summary of optimal hybrid topology (chain first stage, gearbox second stage) based on recommended design rules.

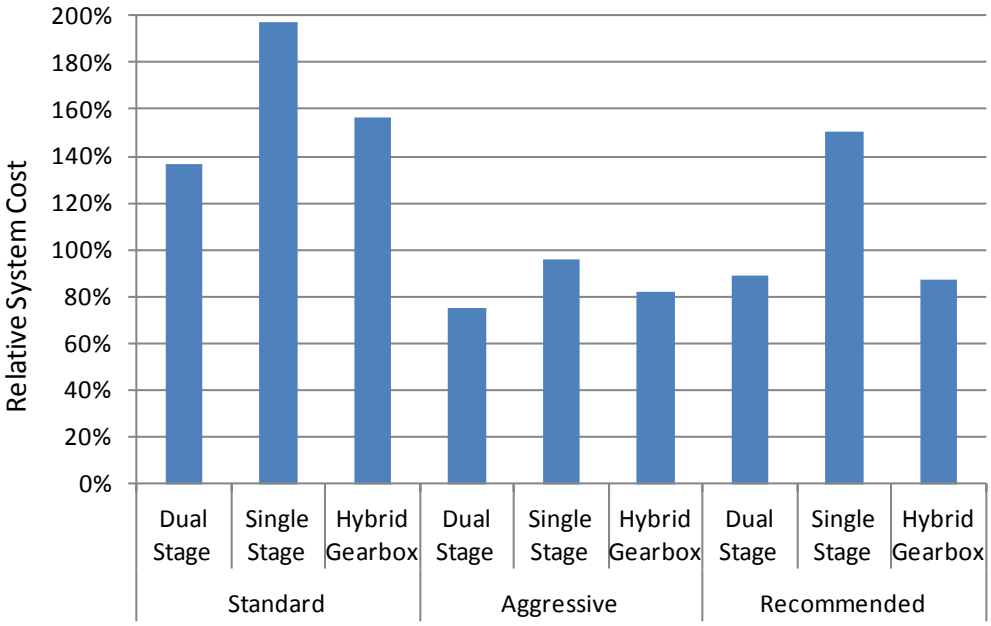

Figure 12: Summary of relative system cost for alternative topologies and design rules.

3.7 Configuration Down-Selection

The top concepts were run through a first-order COE analysis to determine the life cycle costs of each configuration (Figure 13). The optimization using the recommended design rules produced a practical and optimal configuration for each topology. The intention of this first-order COE analysis was to capture and quantify the cost drivers that were not included in the simple parametric modeling. For example, initial estimates for efficiency (AEP) and reliability (LRC) were made for each candidate topology and included.

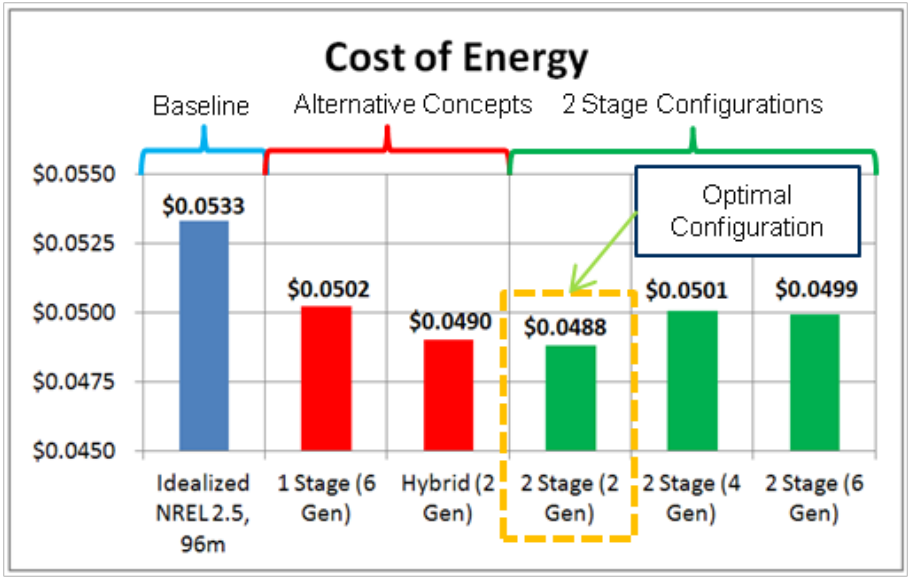

Figure 13: Preliminary COE results of candidates based on the recommended design rules.

The **two-stage dual-output chain drive configuration** showed significant advantages in initial capital cost, annual LRC reserve fund savings through lower part count and lower system complexity, and it yields the lowest total cost of energy. This configuration was selected for further detailed analysis at the component level (Section 4) and the product level (Section 5). The proposed design relies on technology advancements beyond the simple application of standard off the shelf chain. The following sections describe the sophisticated load, wear, dynamics, and efficiency modeling as well as component technologies that are used to move beyond the current state of the art for this application.

4 DETAILED CHAIN ANALYSIS

4.1 Overview

UTRC developed physics-based models to analyze the underlying cause of possible chain failure, vibration, and wear. These models are divided into three elements (Figure 14). First, a dynamics model was developed to analyze the factors that cause intermittent motion of chain system and define chain system parameters that can improve chain system dynamics, potentially reducing noise and roller-to-sprocket tooth impact (Section 4.2). Second, finite element (FE) analysis of the chain and sprocket interfaces, for both static and dynamic cases was preformed. The static FE analysis predicted the pin/bushing bending stresses and effect of design tolerances on chain component performance, while the dynamic FE model predicted the contact stresses, pressure, slip distance, and contact area (Section 4.3). These data were then used as inputs to the third modeling element, analytical models to predict the chain wear, life, and efficiency (Section 4.4). In addition to providing physics-based estimates of chain wear and efficiency, these analytical models enabled sensitivity analysis to identify avenues for chain improvement (e.g., superior hardness and surface roughness).

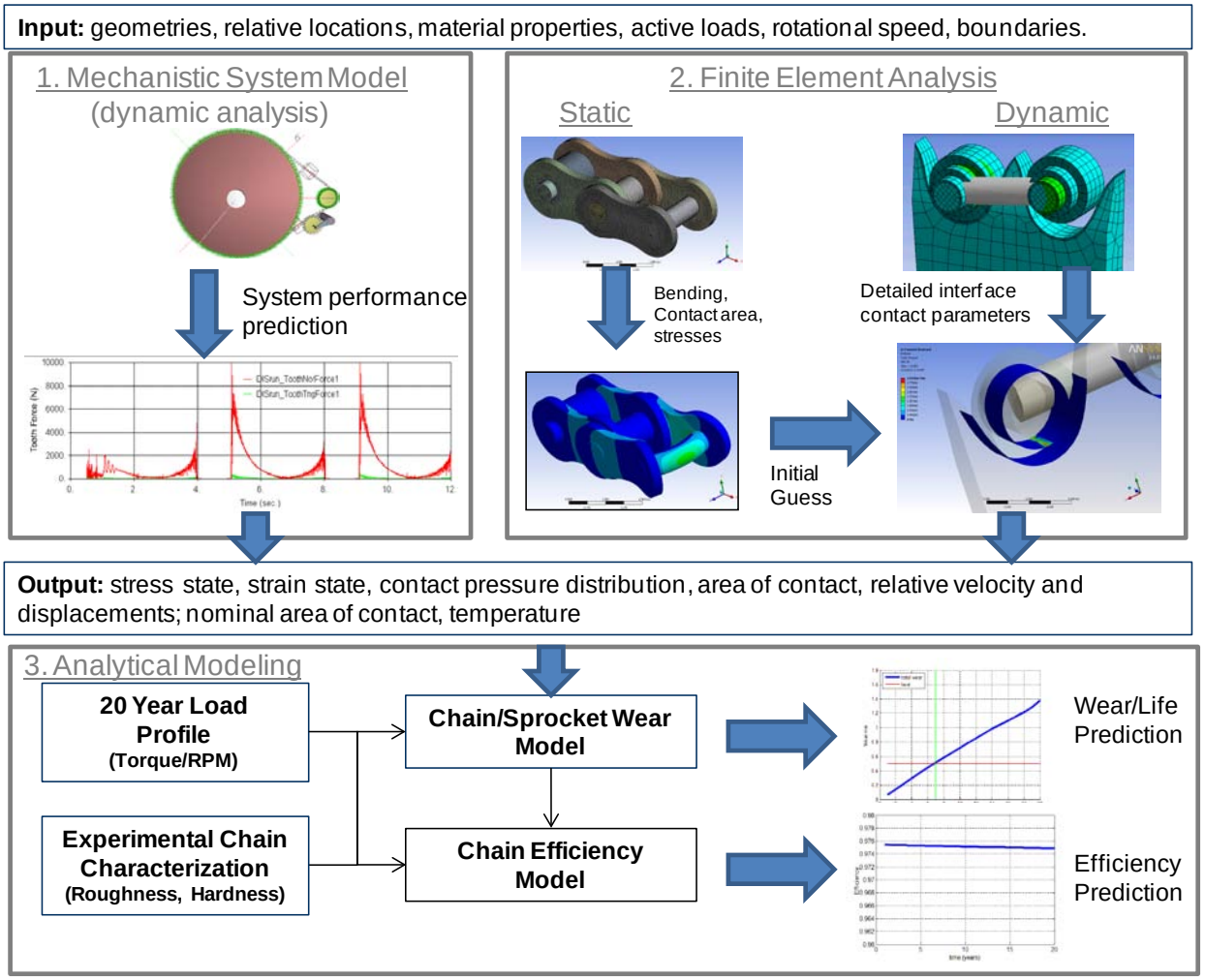

Figure 14: Flow chart of the chain modeling modules used to predict chain life and efficiency.

4.2 Chain-Sprocket Dynamics System Modeling

The Clipper first-stage chain model was implemented by Advanced Science and Automation Corporation using IVRESS (Integrated Virtual Reality Environment for Synthesis and Simulation) [34]. The software is intended for modeling large mechanical systems. The unique strength of this package is that every system element can be represented with a model of variable complexity from a very simple lumped-parameter model to a finite-element detailed model. Furthermore, an important feature of this application is the algorithm it employs for very fast solution of the contact problem. The software has been written in an object-oriented fashion that allows fast and seamless assembly of highly complex system models.

4.2.1 First-Stage Chain Model

A model was created to mimic a single-stage, single-strand chain drive (Figure 15.A) with the potential to be expanded to multi-strand and multi-stage chain drive models. As an output it provides averaged forces and torques on each sprocket tooth and chain link as a function of time. These data are required for UTRC's ANSYS detailed model of the tooth and roller contact and also for space-resolved modeling of the contact stress distribution on the contact surfaces of the chain-sprocket interface.

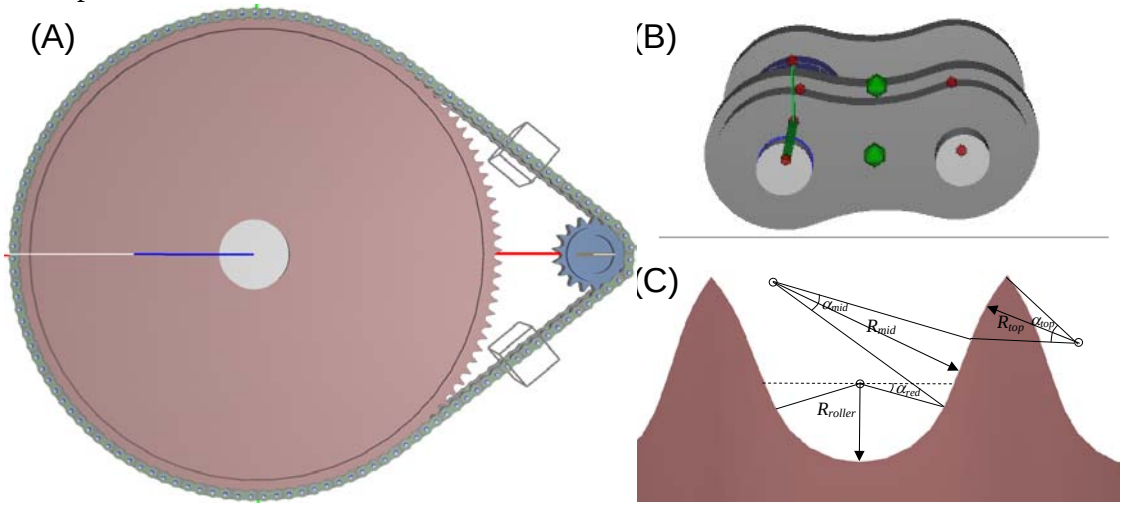

Figure 15: (A) Single-chain dynamics model, (B) chain link model, (C) and sprocket profile.

The chain-pin subsystem has been represented by a lumped model of connected masses and springs as shown in Figure 15.B where the green and the red dots visualize the connection points in the lumped chain model. The model uses the real tooth profile (Figure 15.C) implemented internally according to ANSI standards. A special pre-loading model block allows for chain-sprocket preloading to formulate proper initial conditions for the transient simulation.

4.2.2 Transient Results

Figure 16 shows the modeling results for 10 seconds of physical time for the low and high chain tension sides. The initial two seconds corresponds to a preloading stage. The chain vibration is evident from the plot. Figure 17 presents Fourier analysis of the high and low tension data from Figure 16. Whereas the low tension vibration is random, the high tension side possesses a structure, some peaks being associated with engagement and disengagement tooth events as the tooth goes around the small and the large sprocket. Figure 18 shows the normal load on the teeth of the small sprocket, including a close look at the normal force profile of a tooth as it passes through one revolution from the low to the high tension side.

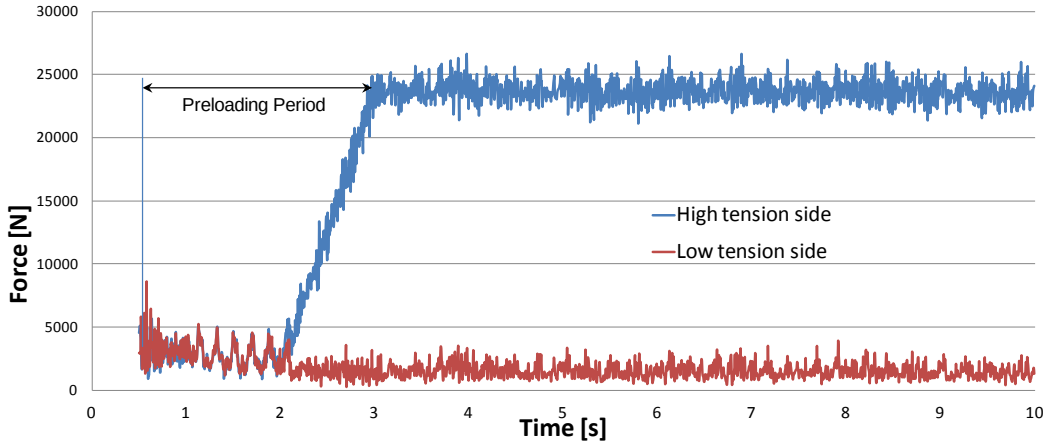

Figure 16: Transient results for 10 seconds of physical time of the chain dynamics model.

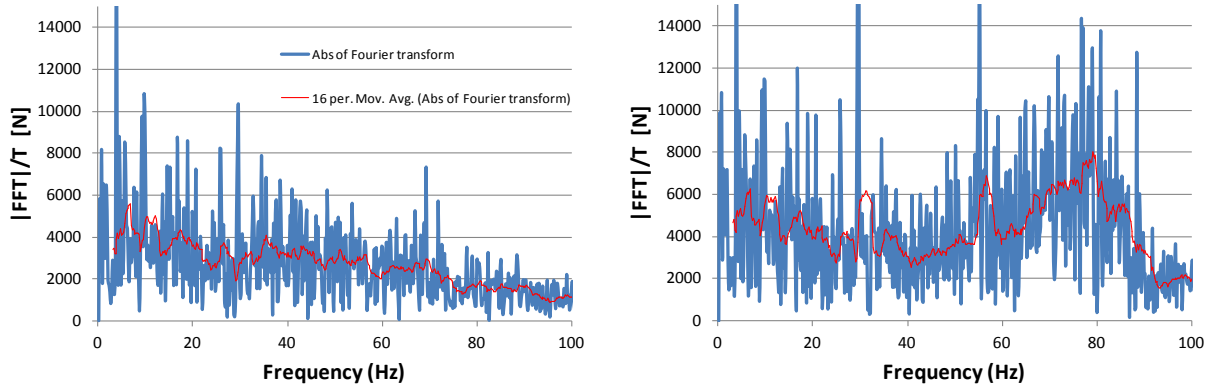

Figure 17: Fourier spectrum of the (a) low tension and (b) high tension side.

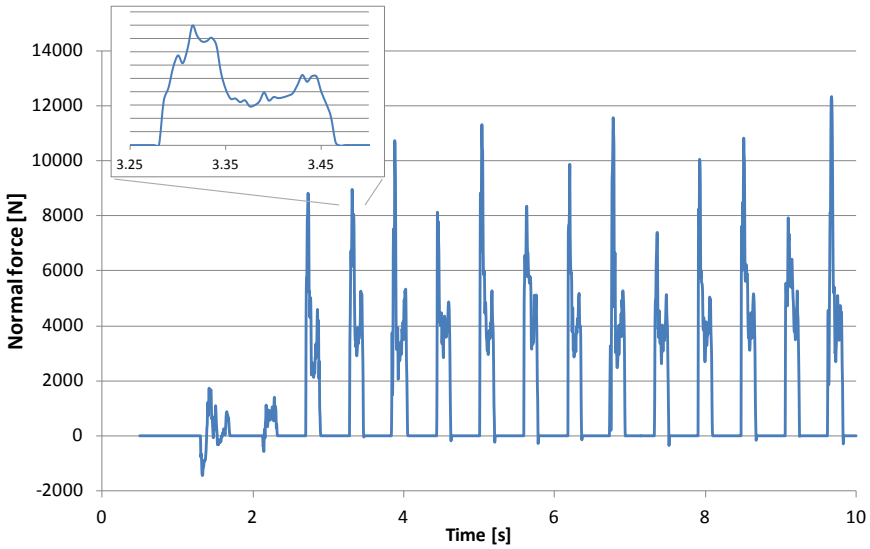

Figure 18: Normal force on the teeth of the small sprocket. Inset: A tooth load of the small sprocket as it goes from the low to the high tension side.

4.3 Finite-Element Modeling of Chain-Sprocket System

To develop life and wear predictions detailed knowledge of normal and shear stresses and sliding distances of the contact surfaces is required. To provide these data a transient model of contact between the chain, pin, bushing, roller, and sprocket was created (Figure 19). Solving these types of contact problems requires significant mesh resolution of the contact surfaces and substantial computational resources. To reduce the computation effort to an acceptable level a number of approximations were made.

First, the simulation time was limited to the first 50 ms of the roller engagement event. This covers 1.5 tooth engagements on the large sprocket, which is sufficient to calculate the highest stress values between the chain and the sprocket. As the chain sprocket system model shows (Figure 20) the maximal loads take place at the moment of engagement and disengagement of the chain roller with the sprocket, the engagement event having the higher amplitude.

To further reduce computational requirements, only a two-tooth sector of the sprocket was modeled, allowing a drastic reduction in the number of mesh cells. The link between the two pins was approximated as a bar with the equivalent stiffness of the actual link. The high tension portion of the chain was modeled as a spring with an effective stiffness of the chain. It was attached to the pin of the engaging roller with the other end loaded with the constant force correspondent to the high side chain tension. To approximate the correct force acting on the engaging roller, the second, already engaged roller was fixed in its position in the sprocket. The plane of symmetry perpendicular to the sprocket axis of rotation has been used to reduce the model size. The mesh was concentrated on the contact surfaces using the boundary layer meshing option. With all the above simplifications the model shown on the Figure 19 runs in approximately 5 days on a 10-processor parallel computer.

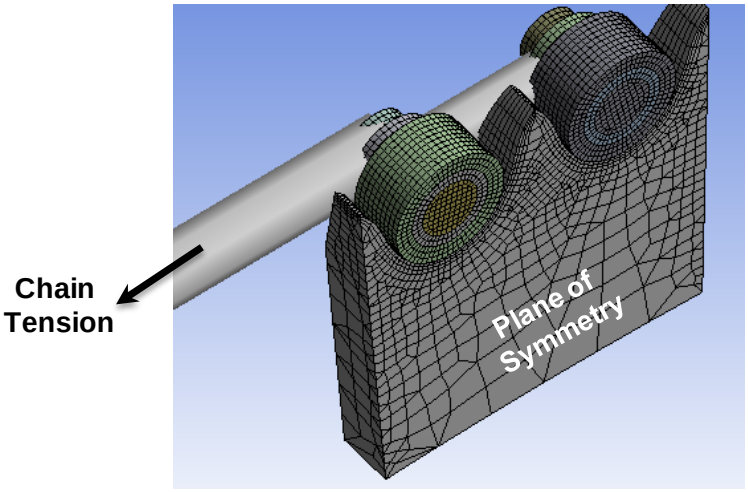

Figure 19: Simplified model of the sprocket sector and chain segment.

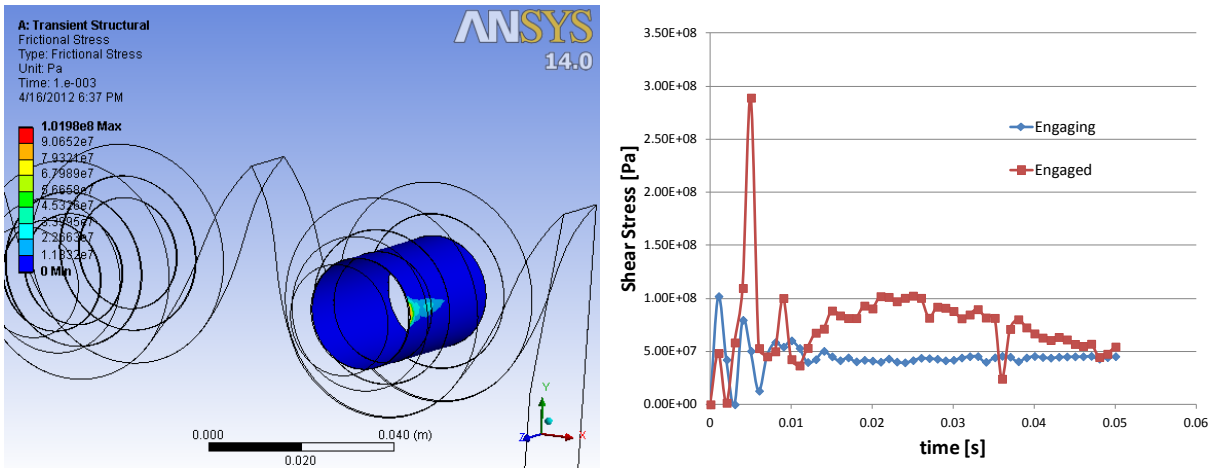

Figure 20: Shear stress between the pin and the bushing at the first microsecond of engagement event (left) and over time (right).

The model traces the evolution of the contact point from the moment the roller hits the sprocket for the first time until the moment it finally settles on the sprocket surface. The details are very sensitive to the actual tolerances between all chain elements as well as damping and stiffness of the materials. Custom scripts were written to extract the detailed nodal information on the stresses and sliding distances of the contact surfaces to be used in the life prediction model.

4.4 Wear and Efficiency Modeling

The objective of this work was to provide physics-based estimates of wear and efficiency for the chain design by investigating the behavior of the chain contact interfaces. Achieving this requires the definition of contact interface based on the kinematic and dynamic properties of the chain. The drive chain consists of a series of journal bearings (pin/bushing and bushing/roller). The surfaces at the interface are case hardened for both wear resistance and toughness. For heavy-duty chain, even under flood lubrication conditions, the high contact pressure and oscillatory motion during articulation will prevent hydrodynamic lubrication between the pin and bushing components [5-8] leading to an increase in their surface wear. The wear of the pin and bush causes a direct increase in the chain pitch leading to an increase in the chain length in the drive. The maximum allowable elongation depends upon the sprocket design and it is on the order of 1.5% of the original chain pitch for a typical standard application.

Most publications indicate that the relative motion in the chain joint (articulation) is too complex to be simulated by pin-on-disc or other similar standard wear models and characterization methods [9-12]. Experiments performed in [9] indicate that wear was observed on most of the pin circumference and that the wear pattern was more equiaxial pitting indicating that the surface has experienced mild fretting in addition to abrasive wear. This observation was correlated to the relative motion between the pin and bush whilst under full load in the tight span of the transmission. To calculate the wear evolution in the chain, the contact properties at the interface between different elements in the chain drive system during articulations were determined from the FE model. The flowchart of the finite element and wear simulation procedure is shown in Figure 21. ANSYS outputs used for this analysis included area of contact, contact pressure, and slip distance.

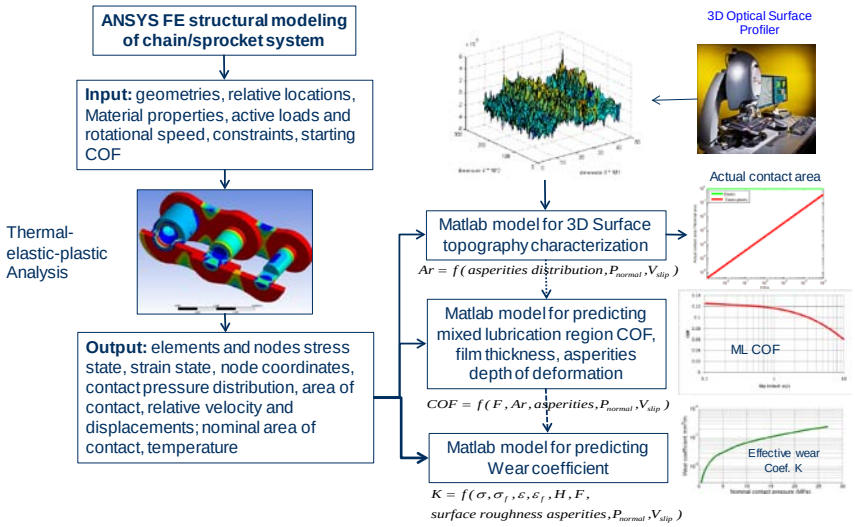

Figure 21: Flow chart of procedure used to predict chain wear.

4.4.1 Prediction of Normalized Contact Area

The contact area predicted from the ANSYS model has to be normalized based on the surface roughness at the interface between each pair. The roughness was measured for each component of standard and high performance chain from a major chain manufacturer. These roughness data were used to predict the ratio between the actual area of contact and the nominal area at the interface between the two components, using the modified Greenwood and Williamson contact model between two rough surfaces (details of analysis can be found in [13]).

4.4.2 Stribeck Friction Model

Most sliding interfaces are lubricated. The friction force will then vary with the sliding speed depending on the extent to which the interacting contact surfaces are running under boundary lubrication (BL), mixed or full-film lubrication. In lubricated chain, the friction decreases with increased sliding speed until a mixed or full-film situation is obtained, after which the friction in the contact region can either be constant, increase, or decrease with increased sliding speed due to viscous and thermal effects (Stribeck friction curve). The friction model is formulated based on the approach presented in [13] as shown below:

$$cof = \frac{F_f}{F_N} = \frac{f_c F_{NC} + \tau_o \operatorname{arcsin} h\left\{\frac{\eta v^{dif}}{h\tau_o}\right\} A_H}{F_N} \qquad \text{Equation 1}$$

Where COF is the coefficient of friction, F_f is the friction force (N), F_N is the normal force (N); F_{NC} is the load carried by the asperities (N); f_c coefficient of friction in the BL regime; A_H total area of the hydrodynamic component in contact (m^2); h film thickness, separation (m); τ_0 Eyring shear stress (Pa); ν Poison ratio; η viscosity (Pa.s). Several case studies from lubricant data are available in the open literature [13, 14] and the measured surface roughness were used to predict the COF in the mixed lubrication zone. In addition, the COF was also predicted for different surface roughness produced by other machining processes. The results in Table 2 indicate that a better finishing process is required to improve the surface quality at the contact between different chain elements and it is also necessary to select proper lubricants.

Contact Condition	Surface Roughness Ra (μm)	Friction Coefficient
Current	2.7	0.1261
Machined - finish	1.65	0.084
Machined - extra finish	1.3	0.071
Ground	0.8	0.053

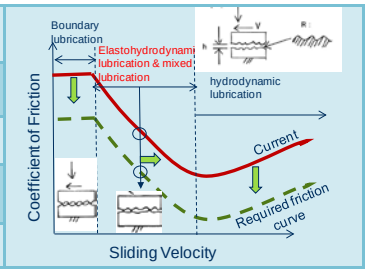

Table 2: Variation of COF with Ra.

4.4.3 Wear Modeling and Prediction

The wear process can be treated as a dynamic process depending on many parameters. The wear rate can be described by a general equation:

{dh/ds =*f (load, velocity, temperature, material parameters, lubrication, …)*}

where h is the wear depth (m) and *s* is the sliding distance (m). Wear models available in the open literature can be mathematically represented in simple empirical relationships or complicated equations relying on physical concepts and definition. Several models representing different wear mechanisms are used to predict the chain components wear and they are listed below [22 - 25]. Limits were set to activate the individual wear mechanisms based on the operating conditions and changes in the surface conditions. The constants for the different equations were obtained for different steel alloys from [22].

Abrasion wear component for lubricated sliding:

$$\frac{dV}{dL} = K\frac{NP_c S_m \alpha}{6\sigma} H * \beta\left[3\sigma exp\left(\frac{S_m}{4\upsilon\tau}\right) - h_o\right]^2 \qquad \text{Equation 2}$$

Melt wear component (surface bulk temperature = melting point):

$$\frac{dV_m}{dL} = A\frac{(T_{melt} - T_o) * H}{(TL_{melt}\beta v_1)}\left(\alpha_{12} f_{Fr} \bar{p} v_1 \frac{T\beta}{T_{melt} - T_o} - 1\right) \qquad \text{Equation 3}$$

Mild-oxidation wear component (flash temperatures >700°C for steel):

$$\frac{dV_{om}}{dL} = A\frac{C_o^2 A_o r_o \bar{p}}{Z_c a_o v_1} exp\left(\frac{E_o}{R_o T_{flash}}\right) \qquad \text{Equation 4}$$

Elongation of chain due to wear is the main parameter that determines chain life. As shown above, the wear rate is dependent on lubrication, load, and the frequency and degree of articulation between pins and bushings. The time history of drive system revolutions and corresponding torque for 20 years was used to determine the expected life of the chain due to elongation. Each data point was used to predict the relation between the main rotor revolutions and the chain link motion, which is controlled by the perimeter length of the chain and the circumference of the large sprocket. A ratio of two main rotor revolutions to one chain link trips around the loop was used.

4.4.4 Prediction of Chain Efficiency

Energy is dissipated during periods of chain link articulation, thus decreasing drivetrain efficiency. The predicted wear depth will affect the energy loss due to the sliding friction. This energy loss can be calculated by summing the integral of the sliding force over the sliding distance at each interface. Using Coulomb's law of friction, the sliding force is proportional to the normal reaction force, which is dependent on the forces in the adjacent chain links and on the orientation of the link [26].

4.4.4.1 Energy Loss Due to Pin Articulation

Frictional losses during the pin articulation are due to the pin sliding against the bush only, and it is independent of the sprocket force. The force on this interface is dependent on the force in the chain span.

$$W_{pin} = \frac{F_c + F_{cf}}{\sqrt{1+\mu_p^2}} \mu_p r_{bi} \alpha_m \qquad \text{Equation 5}$$

4.4.4.2 Bush Articulation

Frictional losses during a bush articulation are due to sliding at the pin/bush interface and either the bush/roller interface or the roller/tooth interface. For a given torque, sliding will occur at the bush/roller interface because it lies at a smaller radius while no sliding will occur between the roller and tooth. The energy loss during a bush articulation is dependent on the seating of the roller and is determined as follows [26]:

$$W_{bush} = \frac{\mu_p F_c r_{bi}\left[\cos\vartheta_{RA} - \cos\left(\vartheta_{RA}+\alpha_m\right)\right]}{\sqrt{1+\mu_p^2}\sin\left(\vartheta_{RA}+\alpha_m\right)} + \frac{F_{cp}\mu_p r_{bi}\alpha_m}{\sqrt{1+\mu_p^2}} + \frac{\mu_r F_c r_{bo}\left[1-\cos\left(\alpha_m\right)\right]}{\sin\left(\vartheta_{RA}+\alpha_m\right)} \quad \text{at tension span} \qquad \text{Equation 6}$$

$$W_{bush} = \frac{\mu_p F_c r_{bi}\left[\cos\vartheta_{RA} - \cos\left(\vartheta_{RA}+\alpha_m\right)\right]}{\sqrt{1+\mu_p^2}\sin\left(\vartheta_{RA}\right)} + \frac{F_{cp}\mu_p r_{bi}\alpha_m}{\sqrt{1+\mu_p^2}} + \frac{\mu_r F_c r_{bo}\left[1-\cos\left(\alpha_m\right)\right]}{\sin\left(\vartheta_{RA}\right)} \quad \text{at slack span} \qquad \text{Equation 7}$$

Energy loss due to chain links offset with an angle γ can be calculated as follows:

$$W_f = \mu_l T_o \sin\gamma \int_{-\alpha}^{0} \frac{\sin\phi}{\sin\left(\phi+\alpha+\beta\right)} r_o d\beta \qquad \text{Equation 8}$$

Energy loss due to the roller rotation on the sprocket teeth to prevent sliding is determined from:

$$W_{fr} = \mu_{rr} T_o r_R \frac{(0.63+/-\alpha)}{\alpha} \int_{-\alpha}^{0} \frac{\sin(\alpha+\beta)}{\sin\left(\phi+\alpha+\beta\right)} d\beta \qquad \text{Equation 9}$$

4.4.4.3 Chain Efficiency

The total loss in the chain drive for a rotation of one pitch can be calculated by summing the losses due to articulation in a two-sprocket drive. The efficiency of the drive can then be calculated:

$$\eta = \frac{P_o}{P_o + N_s \omega_s \sum W} \qquad \text{Equation 10}$$

4.4.5 Results

The changes in the pin diameter, bushing internal and external diameter, and roller internal diameter due to wear were calculated for 20 years load profiles. Wear and efficiency for the selected first and second stage were predicted. The chain life was predicted to be approximately 7 years for the first stage and 11 years for the second stage. The efficiency was predicted to be 98% for the first stage and 99% for the second stage.

5 FINAL PRODUCT CONFIGURATION

5.1 General Overview

Following the results of the optimization study, the **two-output dual-stage chain drive** was selected for further detail design and wind turbine product integration. The general configu-

ration is assumed to be compatible with a representative 2.5 MW baseline. This synergy allows for easy integration and cost comparisons using the baseline rotor, tower, and electrical system.

The final product-level details of the chain configuration are the same as the output of the optimization study (Figure 9) with the exception of the number of teeth on the first-stage large sprocket. The tooth count was changed to make the number of teeth easily divisible by a whole number to create manageable and removable teeth sections. This change had a negligible impact on the total system cost. The overview of the main product configuration and component layout can be seen in Figure 22 and Figure 23. The first stage utilizes readily available 3" pitch 240 ANSI chain and the second stage uses 140 ANSI for a total gear ratio of about 50. It is worth noting that there are larger standard series chains available enabling this concept to be scaled-up for higher-megawatt concepts in the future.

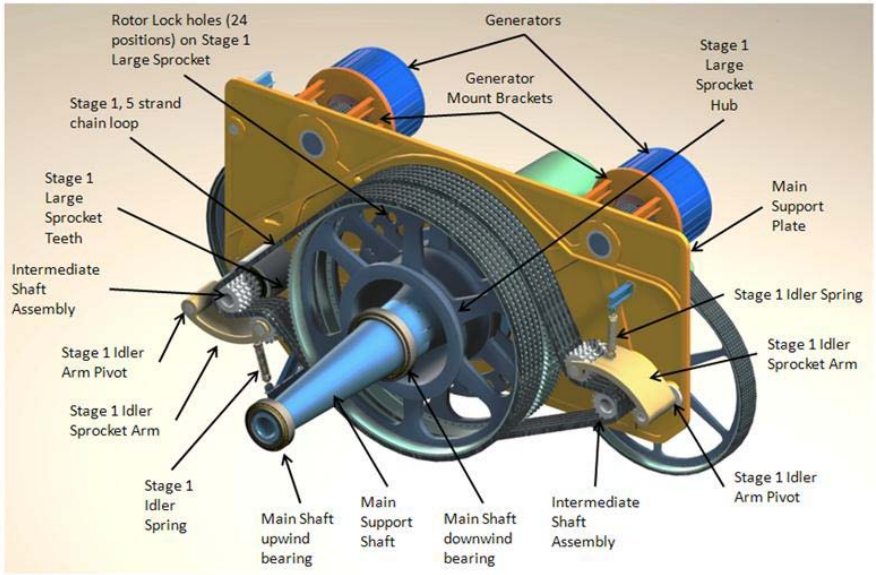

Figure 22: Upwind view of the final product configuration.

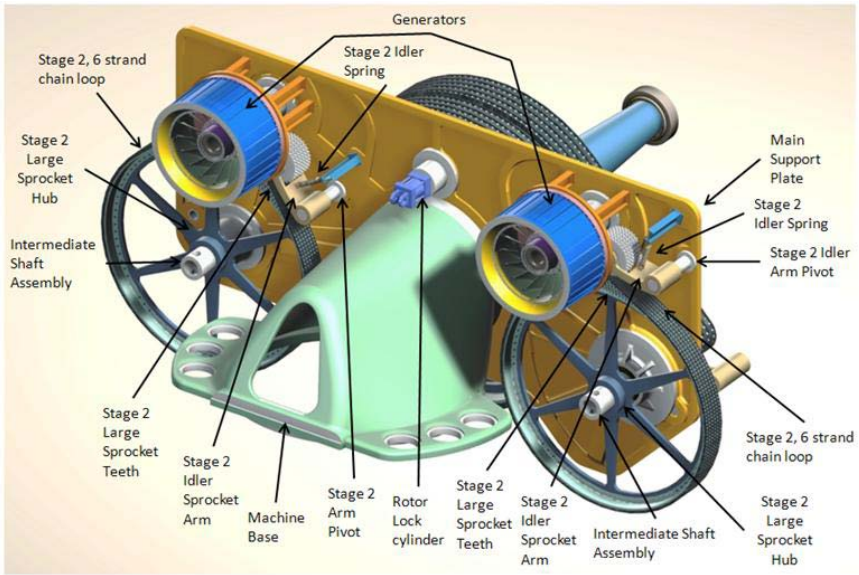

Figure 23: Downwind view of the final product configuration.

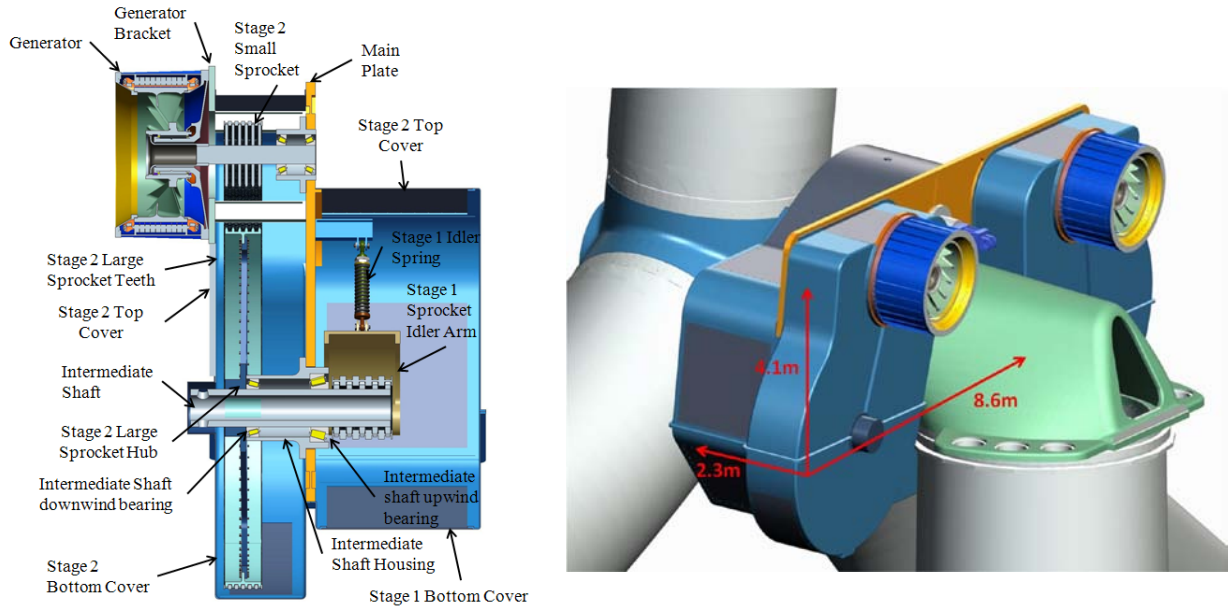

Figure 24: Cross-section view (left) and overall dimensions (right) of the final configuration.

5.1.1 Key Design Features

The chain drive creates many challenges for wind turbine product design. For example, the large diameters and center distances require expansive support structures. However the unique transmission also offers opportunities for systematic change to the design of a drivetrain. Key areas of design enhancement are highlighted below:

Main Support Shaft/Kingpin: The chain strand has inherent flexibility that yields a reduced sensitivity to alignment and off-axis rotor loads. This feature allows for new lightweight configurations of support structures. The large diameter main sprockets and large center distances do not require the use of a standard bedplate common to gearboxes. By using a large center bore, the main sprocket can be outer-rotating and directly mounted to the hub similar to a direct drive generator. This also eliminates an expensive and heavy main shaft.

Main Support Plate: Another advantage of the reduced alignment requirement of chain transmission is the ability to cantilever the sprockets thereby lowering housing structural weight and cost. This is accomplished through designing the main support of the drive sprockets as a central web or plate. The support plate can be a simple part with generous tolerances and simple machined bores as the idlers on each loop take up the slack and accommodate for large positional errors. The central plate support structure also allows for the outer walls to be simple light gauge sheet metal or composite covers as they do not need to support any of the bearing loads.

Cartridge Bearing Support: The sprocket shafts and bearings are housed in individual cartridges that can be easily replaced in case of a failure. The bearing design methodology uses preloaded taper roller bearings in all possible positions, with the exception of the lightly loaded idler shafts. The limited requirement for axial alignment of chain transmissions allows for the use of this locating bearing arrangement in all loaded positions. Preloaded tapers reduce the risk of roller skidding and have proven reliable in the wind industry.

Adjustable Idlers: The idler sprockets are mounted on a pivoting arm that can continually adjust for change in chain length due to wear elongation. This pivoting arm eases installation and removal, as it can also be rotated out of the way.

Segmented Sprocket Teeth: Additional design for reliability is captured in the large sprocket design. The large sprockets have cast hubs with 10 removable sections of sprocket teeth. Should a tooth fail or wear abnormally, some or all of the tooth segments can be easily replaced in-situ using the onboard crane.

Shipping: The overall dimensions of the chain drive system were restricted to 4.1 m wide by 4.0 m high to meet standard transportation requirements. The layout was optimized using the flexibility of the chain drive sprocket arrangement to accommodate these requirements.

Maintainability: The onboard crane can be used to remove the top covers of each stage (see Figure 25) and for handling the chain for up-tower chain removal and installation. The bearings for the output and generator shafts can also be removed and replaced up-tower, with some additional disassembly (of large second stage sprocket or generator) using the onboard crane.

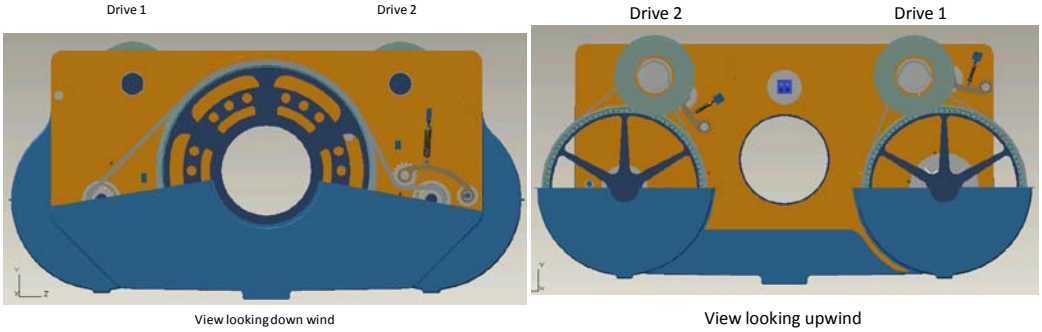

Figure 25: Downwind (left) and upwind (right) views without top covers.

5.2 Finite-Element Analysis

To validate the chain drive design a preliminary finite element analysis (FEA) was performed on all major structural components. Using Nastran analysis software, the FEA process confirmed the structural integrity of critical chain drive parts and allowed for a first-order optimization of these components to reduce size, weight, and estimated cost.

5.2.1 Sprocket Analysis

The first and second stage sprockets are made of ductile cast iron and stress analysis confirms that the sprocket hub design is robust enough to accommodate the loads imparted by the chain drive. The sprocket teeth are fixed to the hub in the form of bolt-on steel segments around the outer rim of the sprocket. The sprocket teeth are of a standard design (ANSI B29.100) and were not analyzed but assumed to be capable of withstanding the chain loading based on published literature and discussions with experienced chain manufacturers. A full analysis of the bolt-on segments along with optimized tooth geometries will be performed in Phase 2 of this project. Stress plots of the first and second stage large sprocket hubs analyzed under the extreme operating torque condition (M_x Max) are shown in Figure 26 below.

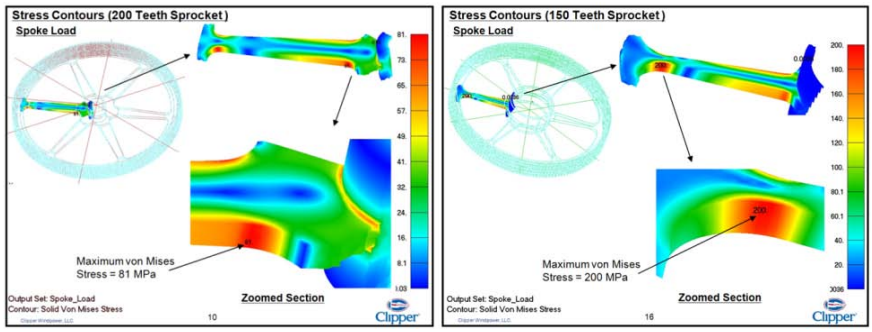

Figure 26: First and second stage Large Sprocket Hub - FE Analysis Results.

5.2.2 Main Support Plate Analysis

The main support plate and bearing housings were also optimized using FEA. The extreme operating torque condition M_x Max was used to evaluate these components. The result of this analysis is shown in Figure 27 below.

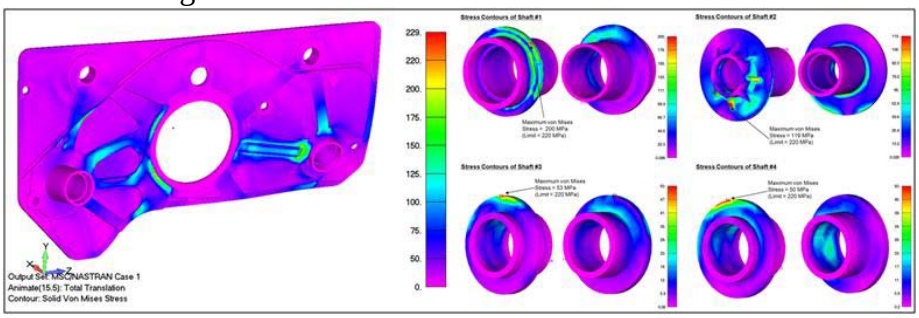

Figure 27: Plate and Output Shaft - FE Analysis.

5.2.3 Results Summary

The allowable stress for ductile iron components is 220 MPa and all of the components have peak stress below the material yield.

5.3 Shaft and Bearing Sizing

The initial shaft and bearing sizing was performed using KISSsoft engineering calculation software. The goals of the KISSsoft calculations are to determine suitable shaft and bearing sizes for cost and weight estimates and are not meant to be final design recommendations. The bearing selections will be discussed with the appropriate vendors and final life calculations will be performed using their proprietary analysis methods in Phase 2. The main shaft and bearings were analyzed using a detailed 652 bin 6-DOF operational and extreme load histogram of torque and off-axis aerodynamic loads. This level of detail ensures that the selections presented here are more than adequate for the design.

The downstream shaft and bearing are sized based on torque and the analysis was performed using full load torque histograms. The bearing lubrication was assumed to be similar to that of the baseline turbine in terms of oil type, delivery, filtration and temperature.

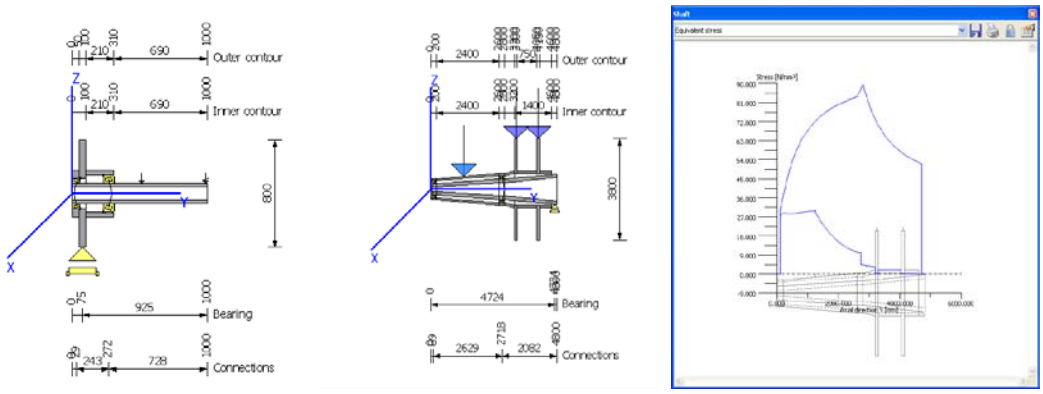

Figure 28: Example KISSsoft shaft and bearing (left) and kingpin shaft (right) calculations.

5.3.1 Bearing Analysis Results

The bearing sizing shows that all bearing selections have more than adequate life and static safety margin. Any excess margin will allow for unforeseen chain dynamic loading, increased reliability or future cost savings.

5.3.2 Shaft Analysis Results

For the intermediate and high speed shafts the shaft diameters were determined by the required bearing bores. In all cases the shaft's loads are low relative to their size and consequently have a very low stress. The kingpin and input shaft are loaded from the aerodynamic moments and the KISSsoft analysis shows the maximum shaft stresses of 90 N/mm^2 are well below the material allowable 220 N/mm^2. All shaft connections will be further validated through detailed FEA in Phase 2.

5.4 Operations and Maintenance (O&M)

The base O&M cost (planned maintenance) for a chain drive turbine is assumed to be equivalent to that of a traditional geared drivetrain, however due to the relatively short life of the chains, these will have to be replaced several times during the operational life of the wind turbine. On average the chains are expected to need replacement every 7 years, before their elongation damages the sprockets or there is a significant chance of chain failure. Both first and second stage chains will be replaced at the same time.

A chain replacement procedure has been developed (Figure 29). Estimates of time and material cost associated with tasks in the procedure were used for the chain drive O&M cost. The chain drive has been designed to facilitate replacement of the chains from the outset. Specialized tools will be designed to accurately join the chains and handle them safely in the restricted confines of the nacelle without the requirement for an external crane and mounting features for temporary access platforms will be included.

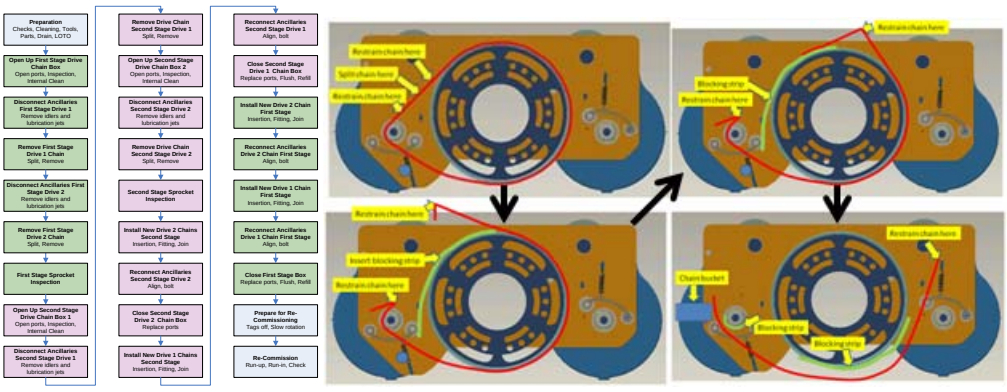

Figure 29: Summary of chain replacement procedure.

5.5 Reliability – Current State versus Chain Drive (LRC)

5.5.1 Reliability Evaluation Methodology

The reliability of the chain drivetrain represents a significant improvement in unscheduled maintenance (or LRC) over that of a traditional gearbox. Published reports state that, industry wide, traditional gearboxes currently have an estimated Mean Time Between Failure (MTBF) of 8.3 years (12% annual frequency of failure). This value was published by ISET and derived from data collected from thousands of turbines operating in Europe [27].

To quantify the reliability benefits of the chain drive relative to the baseline, block diagrams were created for both cases using ReliaSoft's BlockSim software package. This software calculates system reliability based on the methodology prescribed in *IEC 61078 – Analysis techniques for dependability – Reliability block diagram and Boolean methods* [33].

5.5.2 Baseline Gearbox Reliability

The L10 design life (or L1 life for gears) for each gearbox component was assigned to a baseline block diagram and a Monte Carlo simulation was performed to generate an observed failure rate versus time prediction for the baseline topology. This simulation provided the expected frequency of failure attributed purely to expected component wear. Failure mechanisms outside of standard wear do exist and must be considered in all reliability analysis. To account for these alternative failure modes, an additional fixed rate of failure was applied to each component which represents random failures, for instance caused by environmental factors such as an overload, necessitating a gearbox replacement. In the reliability software package the magnitude of the random failure component was calibrated until a 12% per year observed failure rate for the gearbox was achieved. The baseline topology block diagram and the annual observed gearbox failure rate are shown in Figure 30. It is important to note that all the topologies considered have multiple load paths, however a system failure was defined to occur when there was a failure in any independent load path. Thus any component failure within the gearbox would trigger a replacement of the entire system.

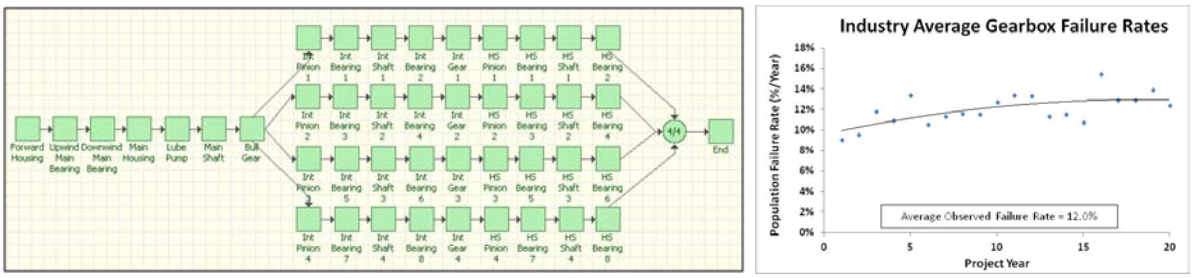

Figure 30: Baseline Topology Block Diagram and Annual Observed Failure Rate.

5.5.3 Chain Drive Reliability

The chain drive turbine has a much higher reliability than a more traditional gearbox for several reasons. First, the chain drive architecture significantly reduces the total number of bearings in the drivetrain system which significantly reduces the annual failure rate. A second source of higher reliability is that other traditional sources of gearbox breakdown, such as gear failures, are eliminated in the chain drive architecture all together. Finally, the regularly scheduled replacement of the drive chain at perscribed 7-year intervals ensures that the chain will always be replaced before its useful life has expired. This greatly reduces the likelihood that chain failure will result in the need for a full chain drive replacement.

To quantify the reliability improvements for the chain drive, a block diagram for the final topology was created using BlockSim and the same methodology described above. For the chain drive bearings, the expected L10 lives were determined through a KissSoft analysis (Section 5.3) and applied to the model. The L10 lives for additional components (shafts, housings, etc.) is assumed to be significantly longer than the 20-year expected life of the turbine. Failure of these components is included in the reliability analysis for completeness but have little influence on the final system reliability outcome as a result. To account for unexpected random failures, the same additional failure rate as used for baseline components is applied to the chain components as well.

This failure rate is significantly lower than the gearbox wear rates due to the benefits of the chain drive. The average annual frequency of failure is calculated to be 4.8% which represents a MTBF of 20.7 years.

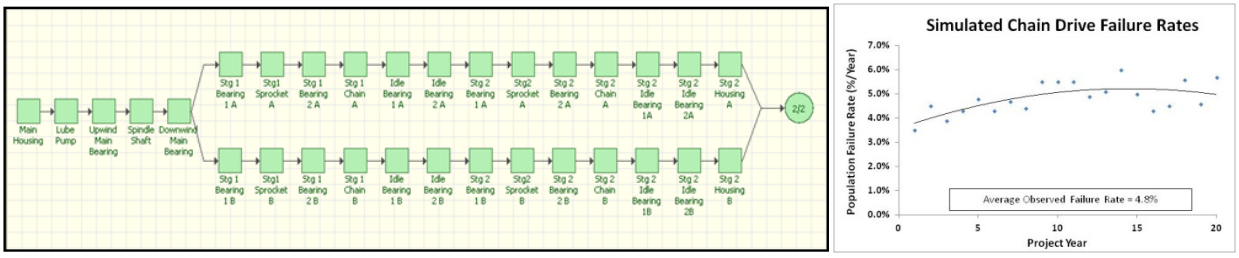

Figure 31: Baseline Topology Block Diagram and Annual Observed Failure Rate.

5.5.4 Generator Reliability Comparison

The annual frequency of failure for a standard wind turbine generator is also assumed to be 12% from the ISET study referenced in Section 5.5.1 above. Chain technology investigated in this report is not intended to address the failure rates of standard generator technology and it is therefore assumed that each generator on the chain driven turbine will have an identical failure rate of 12%.

The topology of the chain drive turbine does however yield some benefit for system level generator reliability. The chain drive turbine has two output generators versus four for the stand-

ard baseline technology. As a result each chain drive wind turbine will require less frequent generator replacements (although at a higher cost per occurrence) than the baseline geared turbine. BlockSim predicts that each chain drive turbine will require an overhaul of a generator every 4.3 years on average versus 2.2 years on average for the baseline turbine.

5.5.5 Reliability Comparison Summary

A complete summary of the reliability improvements for the chain drive relative to the baseline turbine is shown in the table below.

Table 3: Summary of bearing calculations: designation, life, and requirements.

Description	Units	Baseline	Chain Drive	% Improvement
Speed Increaser Freq. of Failure	%/Year	12.0	4.8	60%
Speed Increaser MTBF	Years	8.3	20.7	148%
Generator Frequency of Failure	%/Year	12.0	12.0	0%
Generator MTBF	Years	8.3	8.3	0%
Number of Generators	#	4	2	50%
Generator System Freq. of Failure	WTG%/Year	46.3	23.2	50%
Generator System MTBF	Years/WTG	2.2	4.3	100%

5.6 System Efficiency – Current State versus Chain Drive

System efficiency is another important consideration of the chain-based drivetrain. The losses due to the surface contact of the chain rollers, bushings, pins, and sprockets were considered in the detailed analysis presented in Section 4.4. In order to determine the total drivetrain system efficiency the losses from bearings and lubrication pumps were also calculated. This total efficiency is compared to the baseline 2.5 MW geared drivetrain calculations to determine the change in AEP for the calculation of COE. The efficiency calculations show that the increased mechanical action and contact surfaces of the chain drive result in a net efficiency loss of approximately 1.8% at rated power.

The chain and sprocket system accounts for the largest reduction in efficiency. However, due to lower bearing part count and the reduced speed of the output stages of the chain drive, the bearing losses are lower for the chain system. The bearing efficiency calculations are performed using equations standard as industry practice. The lubricant pump is assumed to be of similar design to the baseline 2.5 MW drivetrain design. Losses for this positive displacement pump were given as a function of RPM from the manufacturer. The chain drive final output speed is lower than the gearbox and the pump uses slightly less energy.

6 COST OF ENERGY ANALYSIS

6.1 Summary of Baseline and COE Assumptions

The Cost of Energy (COE) for the proposed chain drive technology turbine was measured against the COE of a generic baseline turbine that was estimated using the scaling methods outlined in the NREL technical report, *Wind Turbine Design Cost and Scaling Model* [28]. The basic turbine parameters for both configurations are identical: 2.5 MW rating, 96 m rotor, 78 m/s tip speed, 80 m tower, and multi-path drivetrain with multiple generators. Due to the topology similarities between the proposed chain drive turbine and the simulated baseline the only COE components (Equation 11) that vary between the two concepts are the Turbine Initial Capital

Cost (ICC) which includes Turbine Capital Cost (TCC) and Balance of Station (BOS), Operations and Maintenance (O&M), Net Annual Energy Production (AEP_{net}), and Levelized Replacement Costs (LRC) associated with the drivetrain. COE calculation parameters such as Discount Rate (DR), Insurance, Warranty and Fees (IWF) are the same for both architectures analyzed.

$$COE = \frac{(DR+IWF) \times ICC + LRC + O\&M}{AEP_{net}} \quad \text{Equation 11}$$

Initial Capital Cost: The Turbine Capital Cost (TCC), for the chain drive turbine was estimated using a combination of costs from the simulated baseline turbine and Clipper engineering estimates for new components such as chains and sprockets based on FE analysis, CAD models, and industry research. The cost of BOM items that are not directly related to the drivetrain but were required to change from the baseline to accommodate the chain drive architecture, such as main frame and spindle shaft, was also estimated in this manner. While the chain drive was found to be slightly heavier it will be less expensive as the added weight is for lower cost items such as cast iron sprockets and chain which replace more expensive yet lighter high precision gears. The cost of the chain drive is lower than the baseline technology because it is inherently less sensitive to deformations and misalignment and requires less precision and less structural mass. The chain topology proposed in this report also has fewer bearings which reduces cost. Furthermore the large bearing spread enabled by the chain drive's kingpin topology allows for a reduction in size and cost of the main bearings.

The proposed chain drive turbine has cost differences for certain Balance of Station (BOS) considerations, specifically transport and field assembly and installation relative to the baseline technology. The chain drive dimensions are still within standard shipping envelope but the additional weight necessitates a higher capacity trailer with more axles. This specialized trailer is less common and thus incurs greater expense per mile due to lower availability. All other turbine components will have the same transport expense as the baseline but the total cost of transport will increase. For both configurations the generators will be installed to the drivetrain in the field. Since the chain drive has two generators versus four for the baseline the cost of installing generators will be reduced as a result. The combined effect of an increase in drivetrain transport cost and a reduction in field assembly is a small net increase for overall BOS.

The combined ICC including drivetrain and all other TCC and BOS expenses for the chain drive is a slight reduction versus the standard baseline. This small savings indicates that from an initial investment standpoint chain drive technology is cost competitive with traditional geared technology.

Table 4: Summary of initial capital cost and mass changes.

Assumption	Description	% Change
Drivetrain Cost	Cost of drivetrain specific components including: low speed shaft, main bearings, spread increaser, & generators	-10.0%
Drivetrain Weight	Weight of drivetrain specific components including: low speed shaft, main bearings, spread increaser, & generators	+29.4%
Turbine Capital Cost	Estimated cost for all turbine equipment	-2.3%
Turbine Weight	Estimated weight for all turbine equipment	+4.2%
Transportation Cost	Cost to transport all turbine components	+2.3%
Assembly & Installation Cost	Cost for field assembly plus construction during turbine installation	-2.4%
Balance of Station Cost	Estimated investment costs not related to turbine equipment	+0.2%
Initial Capital Cost	Estimated total cost	-1.6%

Levelized Replacement/Overhaul Costs (LRC): This covers any unscheduled overhaul costs for major turbine components such as blades and drivetrain. For this analysis only the overhaul of the gearbox and chain components were considered in depth. The initial driving design factors of the chain drive wind turbine were to reduce COE by creating a low cost compliant system that can handle deflections and misalignments thereby significantly increasing mean time between failures. This design also allows for a decrease in mean time to return to service for many failure modes by implementing replaceable chains, bolt-on sprocket segments, and lightweight small sprockets.

The average MTBF for the conventional gearbox in the baseline turbine is assumed to be once every 8.3 years (12% failure rate [1]) as described in Section 5.5.1 on drivetrain reliability. A high capacity crane is required for the overhaul of the gearbox with a total mobilization cost of $300K. It is assumed that failures of both the baseline gearbox and the proposed chain drive will likely be detected before they become catastrophic in nature and there will be some amount of operating life remaining. Thus there is no immediate need to mobilize a large crane when a failure is detected, enabling wind farm operators to schedule replacements at a time when the crane cost burden can be shared among multiple failed turbines. It is assumed that a crane will be mobilized to the project site after 3 turbines have been identified for replacement. Each gearbox replacement will require an estimated repair time of 6.5 days [1]. For the baseline gearbox the cost per replacement includes all labor, replacement equipment, and associated crane costs as well as the loss in energy revenue due to turbine downtime during the procedure.

Chain drive technology offers significant advantages related to drivetrain replacements and overhauls. Due to the scheduled 7.3-year chain replacement (described in Section 5.5.3 above) a very low rate (3 sigma) of chain failures is assumed. Chain drive components (chains and sprockets teeth) with unscheduled failures can be replaced using an on-board crane and the mobilization of a high capacity crane is not required. The chain drive has fewer components such as bearings and shafts which fail through wear and other environmental factors which necessitate a full system replacement. Through BlockSIM analysis, described in section 5.6, it is estimated that the chain drive will have a frequency of failure of 4.8% (MTBF of 20.7 years) which is a significant improvement relative to the baseline technology. The cost for each chain drive replacement is estimated to be about $100K less than the baseline gearbox including labor, replacement parts, crane, and energy losses. The replacement procedure is significantly lower than the baseline replacement due to the lower capital cost of the chain drive equipment.

Table 5: Unscheduled Speed Increaser Replacement Costs

Assumption	Description	Units	% Change
Speed Increaser Replacement Cost	Cost of a single gearbox/chain drive replacement including labor, parts, crane, and lost energy revenue		-16.7%
Annual Speed Increaser Reserve	Annual reserve fund required for unscheduled speed increaser replacement		-66.4%

Similar to the gearbox, it is assumed that each generator will have a MTBF of 8.3 years (12% failure rate [1]). For both turbines failed generators can be replaced with an onboard crane with 1 day of labor. The generators for the chain drive are assumed to have the same frequency of failure as the baseline technology; however, there are 4 generators on the baseline turbine versus only 2 on the chain drive. The higher population size leads to more generator replacements (but at a lower per unit cost) for the baseline topology than the chain architecture. A summary of the generator replacement costs is shown in Table 6 below.

Table 6: Unscheduled Generator Replacement Costs

Assumption	Description	% Change
Single Generator Replacement Cost	Cost of a single generator replacement including labor, parts, and lost energy revenue	+132.7%
Annual Generator Reserve	Annual reserve fund required for unscheduled generator replacement	+16.4%

The annual LRC cost used in the cost of energy analysis is a composite of replacement cost for the gearbox/speed increaser, the generator, and a general replacement reserve for turbine items. The general replacement reserve fund is estimated as a function of turbine rating as outlined in Section 3.4.1.24 in the NREL Cost and Scaling Model [28]. It is assumed that 50% of this general LRC amount is due to generator and gearbox replacements, this portion has been removed and replaced with the more detailed generator and gearbox LRC values described above. A summary of the total LRC cost is shown in Table 7.

Table 7: Comparison of Drivetrain LRC costs ($k/WTG/year).

Category	% vs. Baseline
Unscheduled General Replacement Cost	0.0%
Unscheduled Speed Increaser Replacement Cost	-66.4%
Unscheduled Generator Replacement Cost	16.4%
Total Annual Levelized Replacement Cost	-42.0%

Operations and Maintenance Costs: The general O&M cost for a chain drive turbine is assumed to be equivalent to that of a traditional geared drivetrain, however due to shorter design life, a standard chain will have to be replaced during the operational life of the wind turbine. From the chain analysis performed in Section 4.4.5 it is determined that the chain will be replaced at 7.25 year intervals. With this replacement schedule drive chains will be replaced twice during the lifetime of the wind turbine.

The O&M cost for the baseline turbine was determined as a function of turbine AEP as prescribed in Section 3.4.1.25 in the NREL Cost and Scaling Model. The O&M for the chain

drive turbine is assumed to be the same as the baseline with the cost of the chain replacement procedure providing an additional annual expense.

A full chain replacement operation can be accomplished in 5 days with a crew of 3 people and the use of an on-board crane. No large crane will be required on site. Each chain replacement procedure (including: labor, new chain, and lost energy revenue) will cost $73K per turbine. Using equations (3) and (4) from Appendix D of the original advanced drivetrain FOA the annual reserve fund necessary for this procedure is $7K per Turbine each year. This $7K/WTG/Year is a cost increase relative to the baseline technology. It is possible that advancements in chain technology could enable a highly engineered chain with a full 20-year life. A summary of the annual O&M costs for both the baseline and the chain drive are shown in Table 8 below.

Table 8: Annual Planned O&M Cost for Baseline and Chain Drive.

Assumption	Description	% Change
General O&M	Scheduled turbine maintenance	-0.6%
Land Lease Cost	Annual lease fees for land used by the wind farm	-0.6%
Chain Replacement	Scheduled periodic chain replacement	N/A
Total Annual O&M	Total annual operating expenses due to planned maintenance, land lease, and expected chain replacements	+8.9%

Annual Energy Production: The annual energy production is calculated using the power curve generated in the NREL Cost and Scaling Model and a hypothetical Class II wind resource with 8.5m/s average wind speeds at 80 meters. The AEP of the chain drive turbine was estimated using the efficiency changes relative to the baseline described in Section 5.6 of this report. For the chain drive slightly lower AEP is generated in Region 2 wind speeds below rated power due to the slightly lower efficiency of chain relative to gears. The AEP_{net} for the chain drive is estimated to be 8,700 MWh versus 8,749 MWh for the baseline. This represents a decrease in AEP_{net} of 0.6%.

6.2 COE Summary and Additional COE Improvements

The chain drive concept **achieves a 10.2% reduction in overall COE**, stemming from a 42.0% reduction in total unscheduled parts replacement costs (Table 7) and a 1.6% reduction in initial capital cost. This is the result of implementing a low cost, serviceable drivetrain.

Table 9: Summary of cost of energy analysis.

Cost of Energy Summary Table		
Cost of Energy Item	Abrv.	% vs. Baseline
Turbine Capital Cost	TCC	-2.3%
Balance of Station	BOS	0.2%
Initial Installed Cost:	**ICC**	**-1.6%**
Levelized O&M Cost	O&M	8.9%
Levelized Replacement/Overhaul Cost	LRC	-42.0%
Annual Operating Expense:	**AOE**	**-27.1%**
Net Annual Energy Production	AEPnet	-0.6%
Cost of Energy	**COE**	**-10.2%**

The proposed drivetrain concept exceeds the DOE next generation drivetrain replacement/O&M cost, and mean time between failure goals (Table 10). Additionally, the chain drive makes substantial improvements in drivetrain deployment cost, a 10.0% improvement versus the

geared baseline when one includes the impact of integrating the chain drive into the wind turbine.

Table 10: Summary of chain drive concept against DOE Next Generation Drivetrain goals.

Next Generation Drivetrain Development Goals		
Objective	Target Improvement	% Change
COE Related to LRC + O&M	-24.0%	-26.7%
Drivetrain Torque Density	50.0%	-21.6%
Torque Volume Density	N/A	-72.5%
Meantime Between Drivetrain Replacement	50.0%	148.3%
Drive Train Deployment Cost	-20.0%	-10.0%
Total Life Cycle COE	-20.0%	-10.2%

The drivetrain torque density and volume density are worse than the baseline, however in our view these metrics are less important since they do not directly influence COE. The chain drive uses large and heavy components relative to a gearbox, however the chain drive envelope has a lot of empty volume and its components utilize low cost manufacturing and materials which ultimately provide a positive impact on COE.

The COE calculations and assumptions above generally consider currently available commercial chain technology; however there are many enhancement possibilities that could offer further step change improvements in COE. Through advanced coatings, hardening, lubrication and other process improvements the design life of the chain could achieve a 20-year lifetime, eliminating any increase in O&M costs (1.0% COE improvement). Advanced designs could potentially increase the already competitive efficiency of a standard roller chain to upwards of 99.5% which would allow for increased energy capture and or reduced component size. These additional configurations and technologies can be studied and optimized in Phase 2.

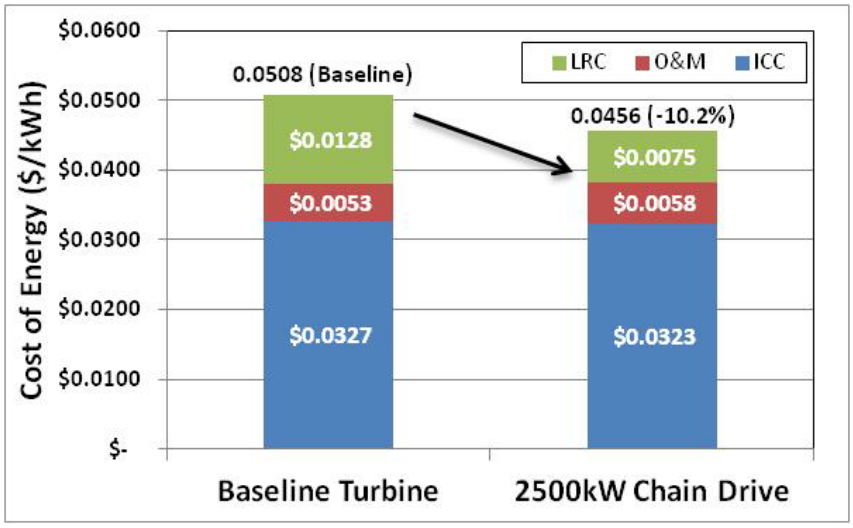

Figure 32: Costs of Energy for NREL-scaled baseline and proposed chain drive technology.

7 RISK REDUCTION AND DEMONSTRATION PLAN

7.1 Key Technical Risk Areas

A risk assessment and risk reduction plan was created. The risk management process involved 1) identification of potential problems, 2) assessment of the probability of those potential problems to occur, 3) assessment of the consequences (to requirements, schedule, and budget) if those potential problems were to occur, and 4) development of a risk-reduction plan. The key technical risks, ranked from highest risk to lowest, along with a high-level summary of risk reduction and risk mitigation actions are shown in Table 11.

Table 11: Key technical risks.

#	Risk	Potential Challenges	Reduction/Mitigation Actions
1	Load Sharing	Inter-strand load sharing factor substantially less than assumed.	Validate load sharing performance on full-scale rig. Enhance through advanced chain (e.g., press fit) or sprocket design if required.
2	Dynamics	Chain strand has unstable dynamic modes, adversely impacting loads and wear.	Comprehensive dynamic system modeling validated by sub-scale and full-scale demonstration units.
3	Unplanned Maintenance	Chain system experiences premature failure.	Dynamic modeling of IEC load cases coupled with coupon and full scale load capacity testing.
4	O&M Impact	Chain replacement and maintenance costs exceed requirements	Validation of chain replacement process and cycle time on full-scale demonstrator.
5	Wear Rate	Wear rates exceed requirements leading to high replacement rates.	Validation of wear model via sub-scale wear HALT rig. Implement commercially proven, replaceable gearbox for second stage if required.
6	First Cost	First cost escalates and is non-competitive. In sufficient supply chain capability.	Track first cost as program key performance parameter (KPP) and engage suppliers and initiate cost reduction efforts as required.
7	Noise	Chain drive noise exceeds existing drivetrain approaches	Measure drivetrain noise on subscale and full-scale demonstrators and mitigate (mistuning sprockets, abatement, hybrid gearbox) as required.
8	Efficiency	Efficiency of chain substantially lower than assumed leading to larger system and lower AEP	Validate on sub and full scale demonstrators. Adopt superior lubrication and advanced chain designs as required.

The probability and consequence of failure were determined for each identified risk to create a risk cube (Figure 33). This total source of risk is shown in Figure 33.

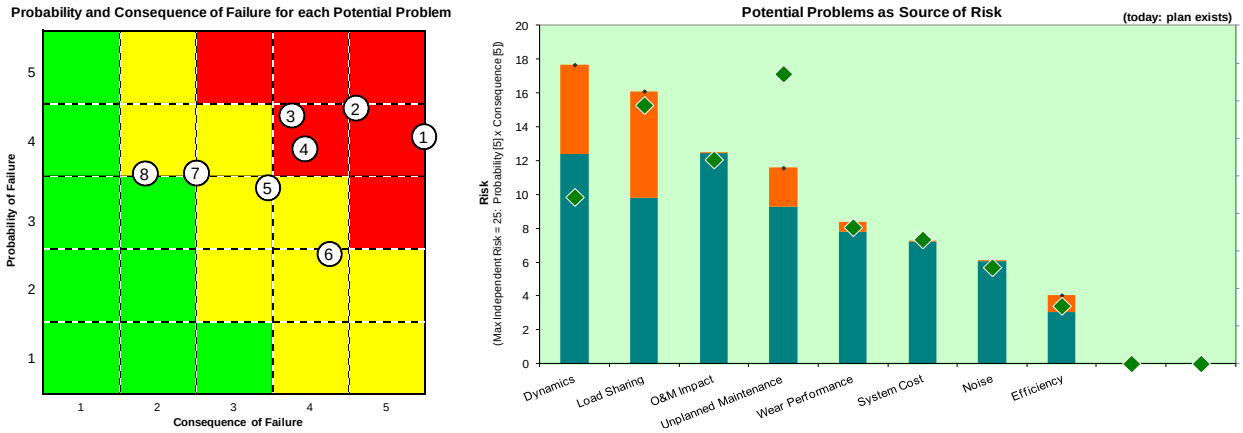

Figure 33: Risk cube for risks identified in Table 11 (left) and overall risk quantification (right).

7.2 Technology Readiness Level (TRL) Analysis

Table 12 lists the major subsystems required for the chain drive system. Technology Readiness Levels (TRLs; based on NASAs definition [29]) are shown for current state and at the conclusion of Phase 2 activities based on the application requirements and operating conditions. While large chain has been used in a number of similar applications no application data exists for large chain at the high torque loads, high tooth count, and long life required for this application. For these reasons we consider the chains and sprockets unproven technology in wind turbine applications. The balance of turbine (e.g., main shaft, bearing assemblies) has been used extensively in wind turbines and Clipper has extensive design, sourcing, and operational experience with these subsystems. To date Clipper Windpower has operated these 'balance of turbine' components on over 730 Liberty wind turbines, accumulating over 12 million operating hours. As such we consider these 'mission-proven' technologies.

Table 12: Technology Readiness Level (TRL) analysis of major subsystems.

Subsystem	Current TRL	Phase 2 TRL	Comments
First Stage Chain	3	6	Target 98% efficiency and 7 year life performance not yet validated. Multi-strand load sharing factor is beyond standard chain design practice.
First Stage Sprockets	3	6	First stage sprocket tooth count is beyond standard chain design practice. Segmented design to be proven at test.
Second Stage Chain	3	6	Target 99% efficiency and 11 year life performance not yet validated. Multi-strand load sharing factor is beyond standard chain design practice.
Second Stage Sprockets	3	6	Second stage sprocket tooth count is beyond standard chain design practice.
Bearings	9	9	Clipper has thoroughly demonstrated with over 12M operational hours.
King pin/Shaft	9	9	Clipper has thoroughly demonstrated with over 12M operational hours.
Generator(s)	9	9	Clipper has thoroughly demonstrated with over 12M operational hours.
Brake/Lock	9	9	Clipper has thoroughly demonstrated with over 12M operational hours.
Machine base/support	4	6	Design uses new central support structure that will require validation and test.

7.3 Risk Reduction Plan

The system risks and subsystem TRL levels were used to define six key tasks (Table 13) that will retire these risks during Phase 2. This is illustrated by the Risk Reduction Waterfall shown in Figure 34, a key output of the risk reduction process.

Table 13: Key Phase 2 risk reduction tasks.

#	Task	Description
1	Coupon link testing	Chain link-level testing to determine articulation wear, load sharing, and ultimate strength.
2	Subscale strand wear rig	Sub-scale, single-strand, rig to run HALT wear tests and initial efficiency and noise measurements for model validation.
3	Dynamic simulation of IEC load cases	Analyze critical IEC load cases to determine extreme dynamic loads on the chain drive (e.g., emergency stop, 50-year gust).
4	FMEA and Reliability analysis	Extend failure mode and reliability analysis to refine life and operational costs.
5	Full-scale prototype test	Conduct full-scale drivetrain test on NREL dynamometer.
6	Cost analysis	Refine cost estimates based on detailed commercialization plan and supply chain engagement.

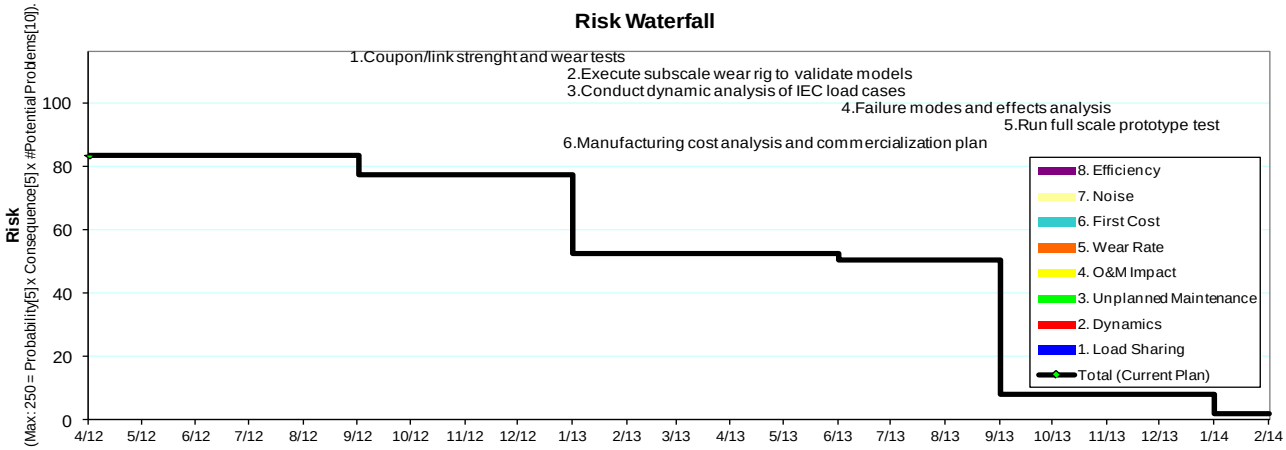

Figure 34: Risk Reduction Waterfall illustrating how the key risks are reduced by Phase 2 tasks.

Details on the sub-scale and full-scale testing are provided in Sections 7.3 and 7.4. A brief explanation of the other tasks is provided below:

Coupon Link Testing: This task would investigate the performance of individual links of chain (both single strand and multi-strand). These tests would characterize: 1) pin and bushing wear rates for prescribed tension loads and articulation angles, 2) multi-strand load sharing, and 3) ultimate tensile strength, either through dog-bone specimen testing or ultimate load testing of single and multi-strand chain segments.

Dynamic Simulation of IEC Load Cases: This task would use the IVRESS code (Section 4.2) in conjunction with the ADAMS multi-body dynamics code to analyze the chain system loads and dynamics when subjected to a full complement of wind turbine dynamic loading. This analysis would cover the full suite of critical IEC load cases [30] and provide refined drivetrain design and demonstration parameters.

FMEA and Reliability Analysis: This task would extend the reliability and structural analyses conducted to date and incorporate the results of sub-scale testing.

Cost Analysis and Updated Commercialization Plan: In this task the results of the Phase 2 testing and design work would be used to develop a refined product configuration capital cost and lifecycle cost. In addition commercialization plans would be developed, including identifying potential field demonstration opportunities.

7.3 Sub-Scale Testing

Clipper Windpower plans to initially develop and test a sub-scale demonstrator for basic validation prior to full-scale testing. Several predictions of friction, wear, and efficiency over the full operating range of the 2.5 MW turbine have been produced. While these physics-based predictions rely upon physical measurements of actual chain hardware for roughness, surface hardness, etc., as input parameters, the predictions will be calibrated using a sub-scale drivetrain test. Testing on smaller scales will enable a lower cost, shorter development time, lower risk effort that reduces first run risk on the full-scale demonstrator. It also provides a platform for longer term corollary testing that may be expensive or time consuming to run on the full scale. As experience with the full-scale article increases, the need for the sub-scale testing will decline. However, follow-on sensitivity tests could be vetted on the smaller platform as concepts for cost reduction or durability improvement are considered.

7.3.1 Sub-Scale Test Objectives

The sub-scale test will focus on wear performance and validation of chain material improvements, and in the process it will also provide initial validation of efficiency, noise, and dynamics. The following list summarizes the test objectives:

Wear Performance: At the sub-scale, the low cost of the test specimens and low cost to operate the rig make it well suited for studying wear performance in a controlled environment. The sub-scale test articles will be run at equivalent conditions as would be expected in the wind turbine application to establish a baseline. A highly accelerated life test (HALT) is envisioned in which the test articles are run at higher speeds and loads to accumulate wear damage cycles at faster rates and hence shorten the test time. The sensitivity of wear performance will be studied as it relates to parameters such as shaft misalignment, lubrication, and load/speed duty cycle. For example, in addition to running in nominal (shaft aligned) conditions the sprocket shafts will intentionally be misaligned in increments to assess the impact on wear performance.

Material Improvement Validation: Various material and finish improvements are under consideration. Individual test articles for the top candidates will be procured and run through a subset of the Wear Performance testing to validate their benefits.

Efficiency: The efficiency performance under the various conditions will be monitored via the shaft speed and torque. Changes of efficiency will also be monitored over time as the chain wears.

Noise/Dynamics: The sub-scale testing will provide an opportunity for initial validation of noise and dynamics performance.

7.4 Full-Scale Demonstrator Testing

The full-scale test article will demonstrate a two stage system using multi-strand chain. The team has elected to save project cost by testing a single leg of the two generator concept. The full-scale test will capture the physics and dynamic effects true to the full scale system, including the effect of operation on an incline to replicate rotor tilt.

7.4.1 Full-Scale Demonstrator Test Objectives

The full-scale test will assess the overall performance of the proposed wind turbine configuration described in Section 5. The test objectives are to validate: (1) deflection compliance and multi-strand load share, (2) noise and dynamics, (3) efficiency, (4) wear, (5) idler optimization and chain life monitoring, and (6) maintainability. The following list summarizes the test objectives:

Deflection Compliance and Load Share: The deflection compliance capability of the chain drive will be assessed by studying the effects of operation under large non-torque shaft loads. The strand to strand load share will be monitored in real time by strain gauges either on the sprocket or chain.

Noise/Dynamics: The dynamics and noise of the two-stage system will be measured. The inertia of the full size components and interaction of the two stages will enable a realistic validation of the wind turbine design.

Efficiency: The efficiency performance of the full-scale system will be measured and compared to the sub-scale data and analytical models.

Wear: Although it is expected that the test duration at the full-scale will not be sufficient to characterize wear performance, the chain will be measured pre and post test to determine the initial wear rate.

Idler Optimization and Chain Life Monitoring: Various material and finish improvements are under consideration. Individual test articles for the top candidates will be procured and run through a sub-set of the Wear Performance testing to validate their benefits.

Maintainability: The full-scale test article will be used to perform a mock chain replacement intended to validate the maintenance procedure. The manpower and equipment will replicate the up-tower maintenance and the time required to complete the process steps will be recorded.

7.4.2 Full-Scale Demonstrator Test Facility

The full scale test will be performed in collaboration with the National Renewable Energy Laboratory (NREL) at their National Wind Technology Center's (NWTC) state-of-the-art dynamometer facilities. The NWTC has two test cells, one rated at 2.5MW and another rated at 5MW, either of which would be suitable for the full-scale test. The facility is uniquely designed to provide the high torque and low speeds typical of a utility scale wind turbine. More importantly, the facility can simulate the large non-torque shaft loads imparted to the drivetrain through the wind turbines large rotor. These features are critical to assessing the real life performance of the proposed drivetrain. Further information about the facilities can be found in reference [32].

7.4.3 Full-Scale Demonstrator Test Article

The test article assembly is a bolted weldment. Future development and production may take advantage of large casting geometries. However, the first article will not be cast out of concern for lead time. The test article represents a single leg of the 2.5MW concept described in Section 5, thus the test article will produce 1.25 MW of electrical power.

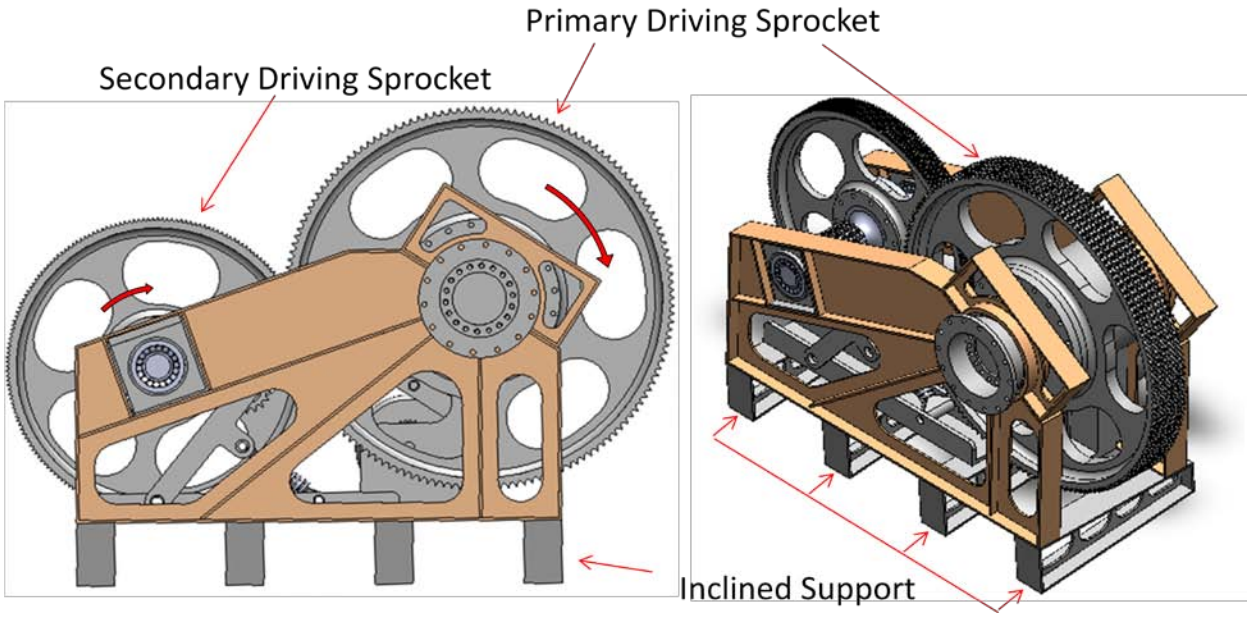

Figure 35: Full-scale 1.25 MW test article (single leg of dual generator 2.5 MW concept). Oil containment shrouds not shown.

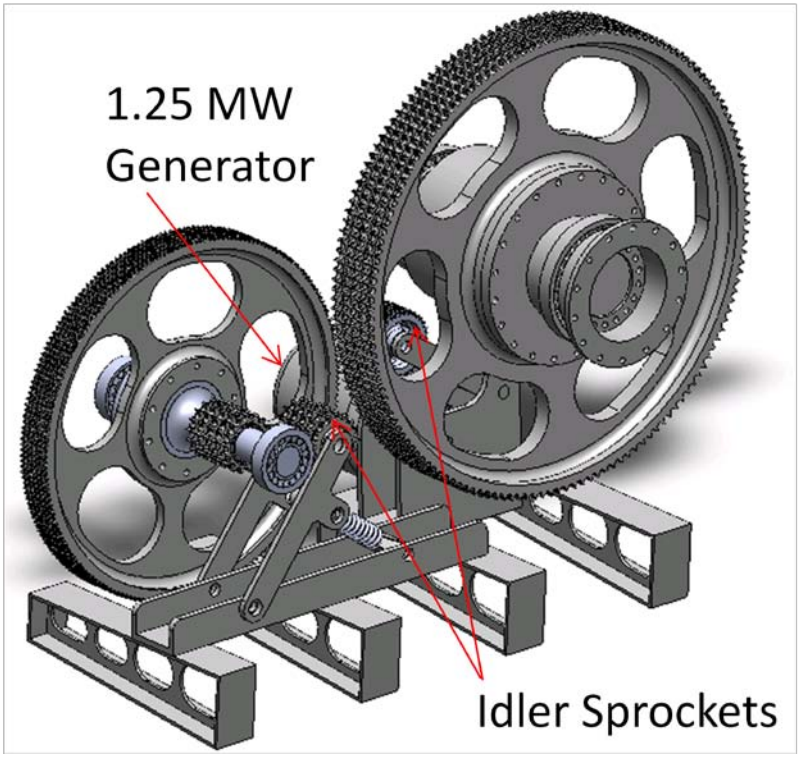

Figure 36: Demonstration unit with major weldment supports removed.

The first stage is mated to the NREL drive motor through a bolted flange. The main shaft supports the large primary drive sprocket. A second shaft carries the first stage driven sprocket as well as the drive sprocket for the second stage. The second stage then drives a generator. With a 15.5 RPM input, the system will provide 781 RPM output to the generator for approximately a net 50:1 speed increase.

The main shaft is set up as a primary datum. The second shaft can be shimmed in two planes at each bearing support to establish baseline alignment. Modifications can be made to study sensitivity to shaft misalignment. Each stage has provisions for a chain tensioner on the slack side of the chain. The system will be studied for sensitivity to tensioner stiffness, preload, and damping.

7.4.4 Full-Scale Demonstration Test Plan

Test planning begins with detailed mechanical and control system integration and safety system design review. Mechanical installation will require setup and alignment checks of the transmission assembly as well as alignment of the system to the stand. Multiple sensing systems will be incorporated both as validation data streams as well as for safety.

For each sprocket, two Hall Effect sensors will be placed in close proximity to both the sprocket and the chain to give objective indication of the chain dynamics. The difference between these sensors will be used with limits set as a safety feedback to the control system. Both 'Operator in the loop' monitoring and automatic exceedance shutdown can be employed.

The primary stage of the full-scale chain drive system will also be monitored via wireless strain gage on the outer links. This also provides excellent validation data for the dynamic simulations, while also adding another layer of safety for running the test article.

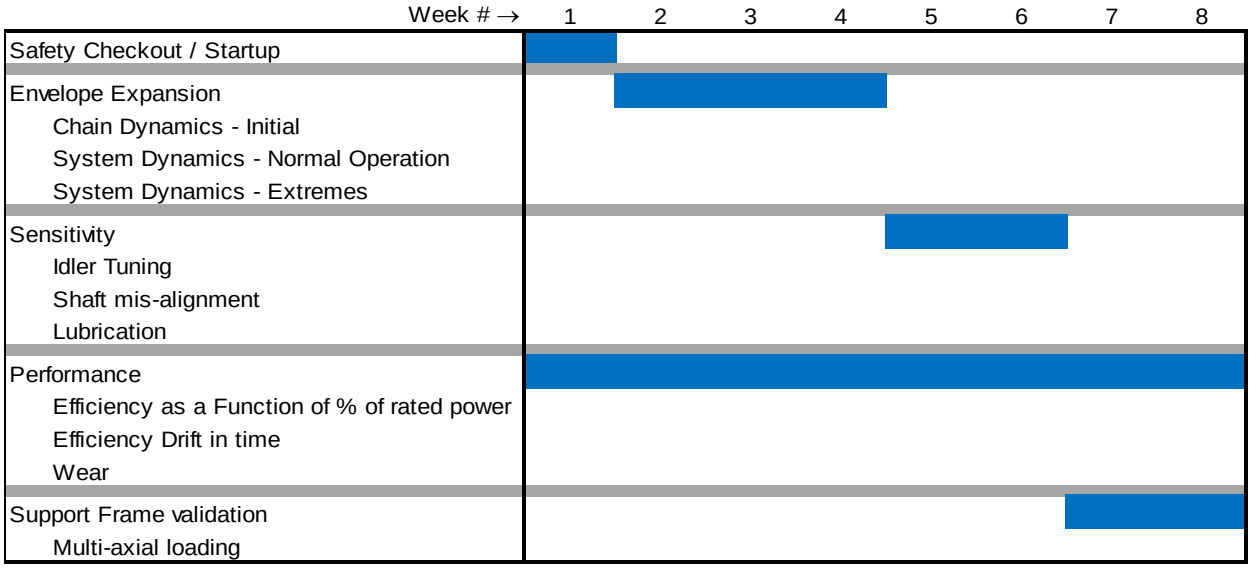

Figure 37: Full scale test schedule.

Figure 37 provides a schedule with several test objectives. After initial checkouts, testing will scan various speeds and power levels following a typical power versus hub speed profile. The expansion of the operating envelope will follow a methodical, gated process starting at low speed and power. Initially, care must be taken to properly reduce the drive power as RPM is decreased so as not to overload the chain drive. Over the test program, this envelope will expand to represent the full range of normal and extreme rotor torques.

As the range of steady operation is expanded, the dynamic characteristics of the chain transmission during slow transient sweeps will also be documented. Once performance under steady and slow transient operation is well demonstrated, more rapid transients will be testing including normal and emergency shutdowns. These will be explored over a range of severity, building confidence in the dynamic response of the system up to and including grid loss simula-

tion. Further integration with NREL will be required to develop appropriate dynamic load profiles for rapid transients since hub and rotor mass and inertias are not presently included.

The NREL drive facility can ensure safe shutdown of the input energy to the primary drive sprocket system. Should a mechanical failure occur downstream, the generator load will act as a means of braking. If required by safety board review, an additional braking system may be added to the first article. Limits will be established for maximum rate of change of key parameters such as hub speed and resistive load torque.

Throughout the program, validation of system efficiency will be a major objective. These measurements will be monitored continually at moderate to low data rate using drive and load power measurements, sufficient to detect 0.5% energy losses or better.

While significant wear is not expected during the short test span, the initial wear-in period will be monitored. Elongation will be observed periodically on shut down measuring pin-to-pin centerline spacing across a predetermined pair of pins in each stage. These pins will not be less than 10 links apart to increase the accuracy of the measurement. It will be necessary to jog the system forward to bring these gage pins into the tension side of the chain drive. A predetermined, very low level static torque will be applied to ensure slack is taken out in a controlled manner. The torque can be applied manually with the drive system locked out. This measurement must be made initially and likely once or twice a week after shutdown. In addition to this manual approach, several dynamic monitoring schemes have been proposed and at least one will be employed for continuous monitoring.

With a successful initial full-scale demonstration, sensitivity to other parameters may be explored, including shaft misalignment, idler tuning and lubrication sensitivity. Each can be changed while monitoring efficiency and chain dynamic responses (noise, vibration, temperature, Hall Effect sensor response, link strain). The short term testing may indicate the system is tolerant of misalignment.

Idler spring dampeners will be optimized for performance. Experience may dictate that the idlers are unnecessary and may be eliminated in production. Several scenarios are possible:

1) Wear is adequately low that automatic adjustment is not required.
2) Adjustment is seldom required manually, but the system is insensitive enough to misalignment that adjustment may be made in the field at the sprocket shafts rather than employing an idler.
3) The system requires automatic adjustment and sprocket shaft adjustment is best performed once as a precision alignment.

The best path through these options is a decision that will be better informed by test. The current approach of including the idlers gives the most flexibility in the test.

7.5 Revised Phase 2 Plan and Schedule

7.5.1 Project Management and Team Structure

Clipper Windpower will lead the project organization (Figure 45). In addition to project management, Clipper Windpower is responsible for tasks involving: (1) cost of energy analysis; (2) concept and prototype design; (3) prototype procurement and assembly. UTRC will focus on structural and contact mechanics analysis of the chain drive, and sub-scale testing and analysis of the chain efficiency and wear performance. Advanced Science and Automation Corporation and Sentient Corporation will support UTRC in the advance chain dynamics, failure, and wear modeling. NREL will conduct the full-scale prototype testing at their dynamometer facility.

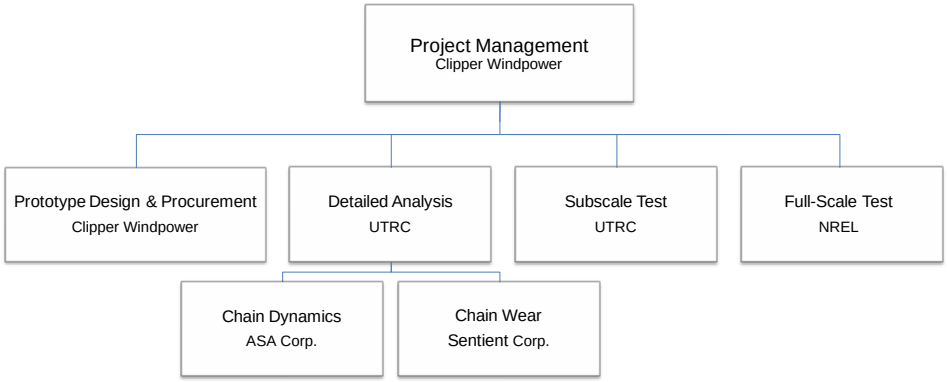

Figure 38: Project organization diagram.

7.5.2 Tasks to Be Performed

Phase 2 tasks as originally proposed in Clipper's FOA application are listed below. Additional scope is shown in **bold**. Explanations of other changes are annotated in *italics*.

Task 7: Detailed Design and Analysis of Full-Scale Test Rig
Based on a favorable "Go" decision by the DOE at the end of budget period one, Clipper shall perform detailed component structural design and analysis of the final prototype design. **This will include a full systems loads analysis cycle assessing the drivetrain's ability to withstand critical IEC loads.** These components will go through a design review process prior to release and procurement of a prototype for use in a large scale dynamometer test at the National Renewable Energy Laboratory.

Task 8: Subscale Testing and Evaluation
Based on a favorable "Go" decision by the DOE at the end of budget period one, UTRC shall work with Clipper Windpower to procure and test samples from candidate chain and sprocket vendors. **These tests will include subscale link articulation wear characterization, link-plate dog-bone yield tests, load sharing tests, and a single strand wear rig test**. This information will be compared to industry best practices. This task will provide data-based input to the COE analysis for cost, durability, and safety factor trades **and will be used to validate wear and efficiency models**. *[Note: Original test objectives for this task to determine alloy composition, surface and through thickness hardness testing via micro indenter and surface finish measurement were brought forward into Phase 1]*

Task 9: Full-Scale Prototype Assembly and Testing
Based on a favorable "Go" decision by the DOE at the end of budget period one, Clipper will develop a complete testing and instrumentation plan in conjunction with NREL. Clipper shall procure components and complete final assembly of the multi-megawatt prototype drivetrain at its Cedar Rapids, IA manufacturing facility prior to testing at NREL. NREL shall conduct full-scale dynamometer testing of the prototype at its facility in Golden, CO. This effort shall measure system efficiency, noise, and loads, at a range of power settings and off-axis loading conditions. Clipper shall also conduct a maintainability assessment on the full-scale test rig to verify maintainability and chain replacement assumptions.

Task 10: Updated COE Analysis and Commercialization Plan
Based on a favorable "Go" decision by the DOE at the end of budget period one, Clipper shall conduct an updated cost-of-energy analysis based on the results of Tasks 7-9. This shall include

sensitivity analysis of the cost of low TRL components, analysis of estimated mean time between failure, and an assessment of component and system manufacturing and assembly cost. Clipper shall develop a commercialization plan identifying further required design optimization, risk reduction, and demonstration efforts.

7.5.3 Project Schedule

Figure 46 shows the proposed schedule and milestones that have been identified for the project.

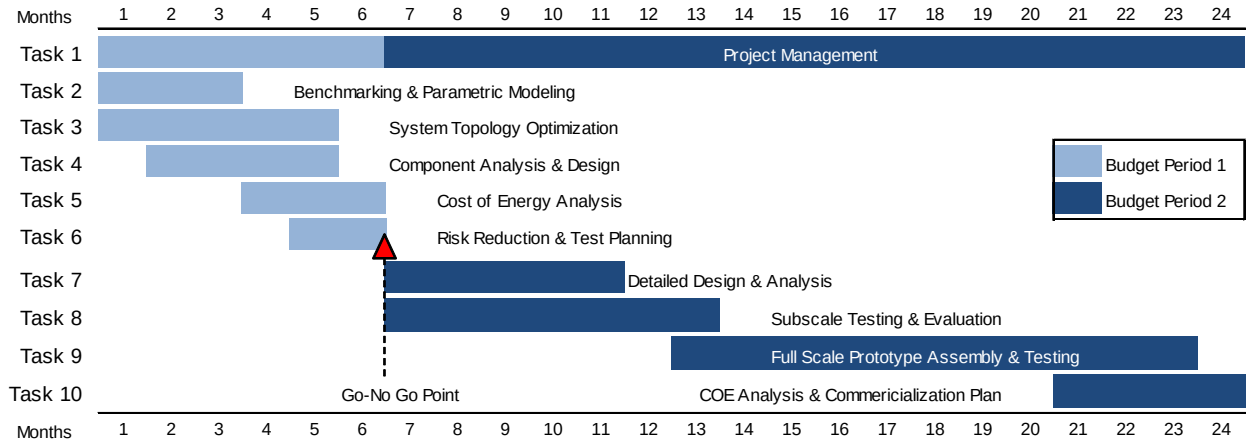

Figure 39: Project schedule Gantt chart with key milestones for the proposed effort.

8 REFERENCES

[1] Asmus, P. and Seitzler, M. "Wind Energy Operations & Maintenance Report" Wind Energy Update, February 2010.
[2] U.S. Department of Energy, Financial Assistance Funding Opportunity Announcement DE-FOA-0000439, U.S. Wind Power: Next Generation Drivetrain Development, Issued 2/7/2011.
[3] Foster, P. "Rare earths: why China is cutting exports crucial to Western technologies", The Telegraph, 19 March 2011. http://www.telegraph.co.uk/science/8385189/Rare-earths-why-China-is-cutting-exports-crucial-to-Western-technologies.html
[4] ASME B29.100, *Precision Power Transmission, Double-Pitch Power, Transmission, and Double-Pitch Conveyor Roller Chains, Attachments, and Sprockets*, ASME, p. 18
[5] Moxon J., "Life determining factors used in chain selection", CME, April 1979, 51-54
[6] Peeken, H. and Coenen, W., "Influence of lubrication on the wear characteristics of roller chains", Proc. 11th Leeds-Lyon Symp. 1984, Butterworth's, 1985, 193-202.
[7] Hollingworth, N. E., and Hills, D. A., "Forces in a heavy-duty drive chain during articulation", Proc. Inst. Mech. Engrs., Pt. C, C5, 1986. 367-374.
[8] Radcliffe S. J., "Wear mechanisms in un-lubricated chains", Tribology Int., Oct 1981. 263-269
[9] Hollingworth, N.E., "A four-square chain wear rig", Tribology International, Volume 20, Issue 1, February 1987, Pages 3-9
[10] Noguchi, Shoji; Yoshiba, Hideaki; Nakayama, Satoshi; Kanada, Tohru, 'Evaluation of Wear between Pin and Bush in Roller Chain', Journal of Advanced Mechanical Design, Systems, and Manufacturing, Volume 3, Issue 4, pp. 355-365 (2009).
[11] N E Hollingworth and D A Hills, 'Theoretical Efficiency of a Cranked Link Chain Drive', Proceedings of the Institution of Mechanical Engineers, Part C: Journal of Mechanical Engineering Science 1986 200.
[12] V. Kerremans, T. Rolly, P. De Baets, J. De Pauw, J. Sukumaran and Y. Perez Delgado, 'WEAR OF CONVEYOR CHAINS WITH POLYMER ROLLERS', Sustainable Construction and Design 2011
[13] Irinel Cosmin Faraon, 'MIXED LUBRICATED LINE CONTACTS', Ph.D. Thesis, University of Twente, Enschede, The Netherlands, November 2005
[14] Matthijn de Rooij, 1998, 'Tribological Aspects of Un-lubricated Deep drawing Processes', PhD Thesis, University of Twente, Enschede, The Netherlands, November 2005
[15] Wikipedia, "Wear," Wikimedia Foundation, Inc., 2010, URL: http://en.wikipedia.org/wiki/Wear.
[16] U.S. Tsubaki, Kyosuke Otoshi, The complete guide to chain, 1997.
[17] S. J. Radcliffe, "Wear mechanisms in unlubricated chains," Tribology International, vol. 14, pp. 263-269, 1981.
[18] American Chain Association, J. Wright, Standard Handbook of Chains - Chains for Power Transmission and Material Handling, Second Edition: CRC Press, 2006.
[19] P. K. D. J. S. Burnell-Gray, Surface engineering casebook: solutions to wear and wear-related failures; Woodhead publishing limited, 1996.
[20] C. R. F. Azevedo, D. Magarotto, and A. P. Tschiptschin, "Embrittlement of case hardened steel chain link," Engineering Failure Analysis, vol. 16, pp. 2311-2317, Oct 2009.
[21] R. E. Melchers, T. Moan, and Z. Gao, "Corrosion of working chains continuously immersed in seawater," Journal of Marine Science and Technology, vol. 12, pp. 102-110, Jun 2007.

[22] Lim SC, Ashby MF., 'Wear mechanism maps', Acta metal, 1987; vol 35, issue #1, pp 1–24.
[23] R. S. MONTGOMERY, 'FRICTION AND WEAR AT HIGH SLIDING SPEEDS' Wear, 36 (1976) 275 – 298
[24] S. Dhanasekaran, R. Gnanamoorthy, 'Gear tooth wear in sintered spur gears under dry running conditions', Wear 265 (2008) 81–87
[25] H.R. Le, M.P.F. Sutcliffe, 'Finite element modelling of the evolution of surface pits in metal forming processes', Journal of Materials Processing Technology 145 (2004) 391–396
[26] C J Lodge and S C Burgess, 'A model of the tension and transmission efficiency of a bush roller chain', Proceedings of the Institution of Mechanical Engineers, Part C: Journal of Mechanical Engineering Science, 2002, pp. 385:394
[27] B. Hahm, M. Durstewitz, and K. Rohrig, "Reliability of Wind Turbines: Experience of 15 years with 1,500 WTs", ISET, 2006: http://www.iset.uni-kassel.de/abt/FB-I/publication/2006-02-09Reliability.pdf
[28] Fingersh, L., Hand, M., and Laxson, A."Wind Turbine Design Cost and Scaling Model", National Renewable Energy Technical Report: NREL/TP-500-40566, December 2006. http://www.nrel.gov/docs/fy07osti/40566.pdf
[29] NASA TRL Definitions: http://esto.nasa.gov/files/TRL_definitions.pdf
[30] Germanischer Lloyd, "Guideline for the Certification of Wind Turbines" Section 4.3, 2010.
[31] Metal Pages Website, April 2012, URL: http://www.metal-pages.com/
[32] NREL Website, April 2012, URL: http://www.nrel.gov/wind/facilities_dynamometer.html
[33] *IEC 61078 – Analysis techniques for dependability – Reliability block diagram and Boolean methods*, Second Edition, 2006.
[34] Advanced Science and Automation Corp., URL: http://www.ascience.com/.